Current Biology

# Rapid growth preceded gigantism in sauropodomorph evolution

--Manuscript Draft--

| | |
|---|---|
| **Manuscript Number:** | CURRENT-BIOLOGY-D-22-01022R1 |
| **Full Title:** | Rapid growth preceded gigantism in sauropodomorph evolution |
| **Article Type:** | Report |
| **Corresponding Author:** | Jennifer Botha, PhD<br>National Museum Bloemfontein<br>Bloemfontein, Free State SOUTH AFRICA |
| **First Author:** | Jennifer Botha, PhD |
| **Order of Authors:** | Jennifer Botha, PhD |
| | Jonah Choiniere |
| | Roger Benson |
| **Abstract:** | Sauropod dinosaurs include the largest land animals to have walked the earth, mostly weighing 10–70 tonnes (e.g.1,2). Osteohistology suggests that derived physiological traits evolved near the origin of sauropod gigantism, including both rapid and uninterrupted growth from juvenile to adult, with little developmental plasticity1,3,4. This differs from the slower, seasonally-interrupted growth of their direct ancestors, as evident in most non-sauropodan sauropodomorphs, which also show developmental plasticity in some groups. Accelerated, but seasonally-interrupted, growth is present in Lessemsauridae, the sister clade to Sauropoda, which also attained giant adult body sizes (>10 tonnes)5. These observations suggest a correlation between giant size and accelerated growth. However, testing this evolutionary connection has been limited by incomplete understanding of growth patterns in some of the closest non-giant relatives of sauropods. We present the osteohistology of two such taxa, Aardonyx celestae and Sefapanosaurus zatronensis. Both exhibit highly vascularized woven-parallel complexes, with fibrolamellar complexes during early to mid-ontogeny, containing regular growth marks. These observations provide strong evidence for rapid, but seasonally-interrupted, growth with limited developmental plasticity (indicated by the regular-spacing of growth marks). Combined with our review of early branching sauropodomorph osteohistology, these results show that highly accelerated growth rates originated among smaller, non-sauropodan sauropodomorphs weighing 1–2 tonnes, but preceded the origins of giant size (>10 tonnes). Therefore, the capacity for rapid bone tissue formation, a derived aspect of rapid growth seen in sauropods, did not evolve specifically to enable giant body sizes, but may have been a prerequisite for them. |
| **Additional Information:** | |

| Question | Response |
|---|---|
| **Standardized datasets**<br>A list of datatypes considered standardized under Cell Press policy is available here. Does this manuscript report new standardized datasets? | No |
| **Original Code**<br>Does this manuscript report original code? | No |

# Rapid growth preceded gigantism in sauropodomorph evolution

**Jennifer Botha[1,2*], Jonah N. Choiniere[3] and Roger B. J. Benson[3,4]**

[1]Karoo Palaeontology Department, National Museum, Bloemfontein, 9300 South Africa

[2]Department of Zoology and Entomology, University of the Free State, Bloemfontein, 9300 South Africa

[3]Evolutionary Studies Institute, University of the Witwatersrand, Johannesburg, 2050 South Africa

[4]Department of Earth Sciences, University of Oxford, Oxford, OX1 3AN United Kingdom

*** Correspondence:**

Corresponding Author

jbotha@nasmus.co.za

**Keywords: bone microstructure, osteohistology, growth patterns, dinosaurs, Sauropodomorpha, Sauropoda, body size, end-Triassic mass extinction, Elliot Formation, Karoo Basin.**

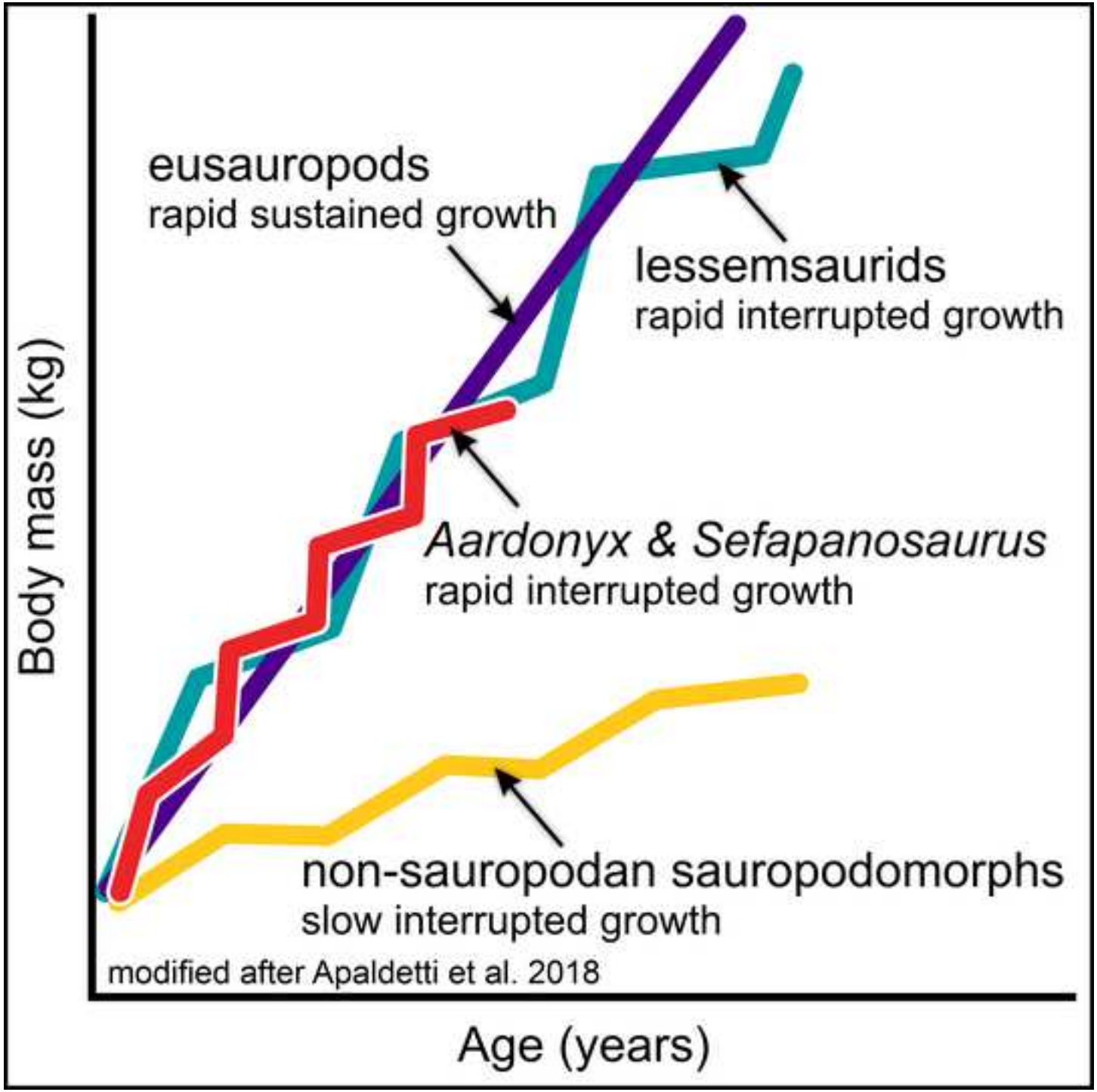

## Summary

Sauropod dinosaurs include the largest land animals to have walked the earth, mostly weighing 10–70 tonnes (e.g.[1,2]). Osteohistology suggests that derived physiological traits evolved near the origin of sauropod gigantism, including both rapid and uninterrupted growth from juvenile to adult, with little developmental plasticity[1,3,4]. This differs from the slower, seasonally-interrupted growth of their direct ancestors, as evident in most non-sauropodan sauropodomorphs, which also show developmental plasticity in some groups. Accelerated, but seasonally-interrupted, growth is present in Lessemsauridae, the sister clade to Sauropoda, which also attained giant adult body sizes (>10 tonnes)[5]. These observations suggest a correlation between giant size and accelerated growth. However, testing this evolutionary connection has been limited by incomplete understanding of growth patterns in some of the closest non-giant relatives of sauropods. We present the osteohistology of two such taxa, *Aardonyx celestae* and *Sefapanosaurus zatronensis*. Both exhibit highly vascularized woven-parallel complexes, with fibrolamellar complexes during early to mid-ontogeny, containing regular growth marks. These observations provide strong evidence for rapid, but seasonally-interrupted, growth with limited developmental plasticity (indicated by the regular-spacing of growth marks). Combined with our review of early branching sauropodomorph osteohistology, these results show that highly accelerated growth rates originated among smaller, non-sauropodan sauropodomorphs weighing 1–2 tonnes, but preceded the origins of giant size (>10 tonnes). Therefore, the capacity for rapid bone tissue formation, a derived aspect of rapid growth seen in sauropods, did not evolve specifically to enable giant body sizes, but may have been a prerequisite for them.


## Results

All the studied bones (see STAR Methods for details) of *Aardonyx celestae* and *Sefapanosaurus zatronensis* display a moderate to very highly vascularized (see Table S1 for quantified vascular density) woven-parallel complex (WPC, Figure 1A, B; Figures S1–3), indicating rapid growth in early-diverging sauropodiforms weighing 1–2 tonnes at adult body mass[6,7]. This complex consists of an interstitial matrix of woven bone, comprising abundant, globular, bunched osteocyte lacunae; and parallel-fibered bone, comprising lenticular osteocyte lacunae evenly distributed in parallel, surrounding the vascular canals to create primary osteons[8]. A slight decrease in zone width towards the sub-periosteal surface of some bones indicate an early to late subadult status for all the elements studied. In some elements, especially those preserving a record of early ontogenetic growth (e.g. Figures 1C, S1A, S1G, S2F), the woven bone is so abundant that the woven-parallel complex forms a fibrolamellar complex (traditionally known as fibrolamellar bone[9] (Figure 1C). This extremely fast growing bone tissue is limited to the inner and mid-cortex (and hence to younger ontogenetic stages). Various elements show a small increase in the incidence of parallel-fibered bone towards the outer cortex indicating a decrease in growth rate with age (Figure 1D, E). All elements exhibit interrupted growth in the form of annuli of parallel-fibered bone, which represent temporary decreases in growth rate, or Lines of Arrested Growth (LAGs), which indicate temporary cessations in growth (Figure 1F, 2A–D, 3). These cyclical growth marks (annuli and LAGs) are typically considered to be annual[10]. None of the bones studied exhibit an External Fundamental System (EFS; also known as Outer Circumferential Lamellae) in the form of numerous closely spaced LAGs and/or an avascular slowly growing region at the sub-periosteal surface, which would have indicated that the individuals had essentially ceased growing (Figure 2E, F). However, there is a slight decrease in the spacing between the growth marks (Figure 3) in some of the bones (e.g. *Sefapanosaurus* humerus BP/1/7434, ulna BP/1/7437, *Aardonyx* radius BP/1/5379a) indicating an overall decrease in growth rate with

age and consistent with our observations of an increasing incidence of parallel-fibered bone towards the outer cortex (see STAR Methods and Supplementary Figures for a detailed osteohistological description of each element).

## Discussion

Bone microstructure of the early-diverging sauropodiforms *Aardonyx* and *Sefapanosaurus* shows a highly vascularized woven-parallel complex with an extremely rapidly forming fibrolamellar complex in the inner and mid-cortices of many of the bones. These observations indicate fast growth rates in early-diverging sauropodiforms, similar to those seen so far in sauropods, the giant near-sauropod clade Lessemsauridae, and the sauropodomorph *Mussaurus*, which exhibits a fibrolamellar complex very early in ontogeny (e.g.[1,5,11,12,13]). Growth marks indicating annual interruptions in growth are present from at least mid-ontogeny, and are fairly regularly spaced throughout the cortex, providing clear evidence for seasonally-interrupted growth similar to other non-sauropodan sauropodomorphs. The combination of rapid, but interrupted growth in *Aardonyx* and *Sefapanosaurus* is most similar, so far, to giant lessemsaurids[5]. However, *Aardonyx* and *Sefapanosaurus* differ from these taxa in showing relatively smaller body sizes at most 1–2 tonnes unlike the > 10 tonne adult body sizes seen in lessemsaurids and sauropods (e.g.[5,14]) (Table S2).

The presence of WPC is typical for Sauropodomorpha and dinosaurs in general[8], but can vary in the proportion of woven bone to parallel-fibered bone. Higher proportions of woven bone are consistent with fast growth rates whereas a predominance of parallel-fibered bone indicates slower growth rates[8,9,15]. Most non-sauropodan sauropodomorphs show a predominance of parallel-fibered bone[11,16,17,18], suggesting relatively slow rates of bone tissue formation compared to sauropods, lessemsaurids and the early-diverging sauropodiforms

96 *Aardonyx* and *Sefapanosaurus* (shown here). The predominance of parallel-fibered bone in
97 non-sauropodan sauropodomorphs also differs from early diverging saurischians such as
98 *Herrerasaurus*[19] and even archosauriforms such as erythrosuchids[20,21] suggesting that slow
99 bone tissue formation had initially evolved from ancestors with faster bone tissue formation
100 around the origin of Sauropodomorpha. Differences between sauropods and other
101 sauropodomorphs led previous authors to suggest that the predominance of woven bone,
102 which indicates fast growth rates, was primarily a sauropodan trait, with a separate
103 evolutionary origin of fast growth rates in the sauropodiform *Mussaurus*[11]. The *Mussaurus*
104 specimens sampled exhibit a mixture of both woven and parallel-fibered bone that was
105 attributed as a possible example of developmental plasticity[11,13].
106 More recently, the osteohistology of the giant (>10 tonne adult body sizes), near-
107 sauropod clade Lessemsauridae has indicated a pre-sauropodan origin for the highly
108 vascularized fibrolamellar complex, indicating that lessemsaurids also exhibited rapid growth
109 rates, similar to sauropods ([5] *Ingentia prima*, *Lessemsaurus sauropoides*). Lessemsaurids
110 exhibit a combination of cyclic growth marks, similar to more basal sauropodomorphs, and
111 increased growth rates more similar to those of the more derived Eusauropoda[5]. The
112 osteohistology from a giant South African lessemsaurid, *Ledumahadi mafube* (approximately
113 12 tonnes), is represented by a senescent individual with a highly remodeled inner cortex.
114 Thus, all that is known regarding this individual is that it exhibited interrupted WPC during
115 mid-ontogeny, growth marks are present at least in the outer third of the cortex and the
116 individual has an EFS[14]. Given that *Ledumahadi* is ontogenetically much older than *Ingentia*
117 or *Lessemsaurus* it is difficult to compare these taxa, and the South African lessemsaurid
118 *Antetonitrus ingenipes* was excluded from this analysis (see STAR Methods for details).
119 Overall, these observations suggest that rapid, but cyclical, growth enabled lessemsaurids to
120 attain giant body sizes prior to the origin of sustained (acyclical) growth in Sauropoda. Our

data indicate that the early sauropodiforms *Aardonyx* and *Sefapanosaurus* also shared these features, differing from the slower cyclical growth of their non-sauropodiform ancestors, and therefore suggesting an earlier phylogenetic origin for this distinctive, pre-sauropodan growth strategy from within Sauropodomorpha.

We investigated the evolution of growth traits on the evolutionary line leading to Sauropoda, undertaking a detailed re-consideration of published osteohistological evidence for early sauropodomorphs (see STAR Methods). Our approach is intended specifically to account for variation in ontogenetic stage among the specimens sampled for some species (see STAR Methods) and the summary of those considerations is presented by taxon in Table S2. This is important because bone deposited during younger growth stages tends to show bone types consistent with faster growth (e.g.[22,23]), and the record or early growth is typically removed or over-written by remodeling in older individuals (e.g.[24,25]). This pattern is evident in the new data presented here, which documents much of the ontogeny of *Aardonyx* and *Sefapanosaurus* across several elements of the skeleton, and also in some previous studies of dinosaur osteohistology (and also see[17,23–29] for similar multiple-element studies).

Previous studies of sauropodomorphs have not been able to effectively account for potentially spurious, age-related variation, due to the more limited data available. For example, Cerda et al.[11] interpreted the bone tissues of *Massospondylus* as being predominantly parallel-fibered, and therefore more slowly-growing than other sauropodomorphs, based on a single, ontogenetically advanced specimen (BP/1/4934). However, ontogenetically younger specimens exhibit a high proportion of woven bone, suggesting more rapid growth during early and mid-ontogeny in *Massospondylus*[18] and Figure S4), similar to other early-diverging sauropodomorphs, including *Plateosaurus* (Nicole Klein, pers. comm. 2021).

We interpreted observations in light of the ontogenetic stage of specimens, assigning taxa to broad osteohistological categories that we then mapped to phylogeny (Figure 4). Our phylogeny is based on the most recent studies on sauropodomorph phylogeny[30–32], and may change pending new discoveries. Nevertheless, key aspects of our phylogenetic hypothesis are conserved among many recent analyses and will likely remain stable[30–32], especially the sister-taxon relationship of lessemsaurids to Sauropoda, and the existence of a clade Sauropodiformes that includes various taxa, including *Aardonyx* and *Sefapanosaurus*, as close relatives of lessemsaurids and Sauropoda.

Once ontogeny is taken into account the first appearance of rapid growth during early to mid-ontogeny (characterized by the predominance of woven-fibered bone in the WPC) appears relatively early in sauropodomorph phylogeny, with *Plateosaurus*, and is shared with *Massospondylus*[18]. However, various basal sauropodomorphs exhibit apparently slower growth, including *Riojasaurus*, *Leyesaurus*, *Adeopapposaurus*, *Ngwevu*, *Coloradisaurus* and *Leonerasaurus*, which exhibit a dominance of parallel-fibered bone or patches of a WPC even in mid-ontogeny (although the sample sizes of these taxa are limited, and thus, some of the bone tissues at different ontogenetic stages remain uncertain, see STAR Methods)[11,30]. In spite of this variation among species, all these non-sauropodiform taxa, including non-juvenile individuals of *Plateosaurus* and *Massospondylus*, document bone tissue types indicative of relatively slower growth compared to sauropodiforms, including *Aardonyx* and *Sefapanosaurus*.

Secondary remodeling in *Aardonyx* and *Sefapanosaurus* is limited to the inner cortex and thus, much of the life history of each individual can be assessed (i.e. ontogeny is not a factor). The zone widths are, however, similar to those of *Massospondylus* (up to 4 mm per zone, 1-2 mm on average), which are narrower than the maximum zone widths seen in *Lessemsaurus* (7.2–13.6 mm, but see above regarding the ontogenetic status of these

specimens) and *Ingentia*. Thus, although their rate of bone tissue formation during the favorable growing season may have been elevated compared to earlier-diverging sauropodomorphs, *Aardonyx* and *Sefapanosaurus* did not deposit the same amount of bone tissue as the lessemsaurids were capable of, perhaps due to a shorter seasonal growth duration. Nevertheless, the presence of a rapidly forming highly vascularized fibrolamellar complex in *Aardonyx* and *Sefapanosaurus* into the early subadult stage indicates that a lessemsaurid-like capacity for rapid bone tissue formation had already evolved in early-diverging sauropodiforms that had smaller body sizes than the Lessemsauridae (Figure 4).

Within a given clade, small taxa grow more slowly than larger members of the same group[33], and thus, body size must be considered when comparing growth patterns. Notably, osteohistological similarities shared by *Aardonyx*, *Sefapanosaurus* and lessemsaurids are independent of overall size given the maximum estimated body masses of 1–2 tonnes in *Aardonyx* and *Sefapanosaurus*, compared to >10 tonne adult body masses of lessemsaurids[5,14]. Therefore, rapid growth rates were present in early sauropodiforms such as *Aardonyx* and *Sefapanosaurus,* prior to the attainment of large body size in the lessemsaurids, indicating a decoupling of the evolution of large body size from that of growth strategy.

Comparisons of the osteohistology of *Aardonyx* and *Sefapanosaurus* to similar-sized non-sauropodiforms also supports the inference that rapid growth in sauropodiforms is independent of body size evolution. For example, non-sauropodiform taxa such as *Plateosaurus* (917 kg) and some *Mussaurus* individuals (1150 kg) exhibit a highly vascularized WPC during mid-ontogeny, with other *Mussaurus* individuals showing a predominance of parallel-fibered bone (e.g. femora MPM-PV 1815[11], MLP 61-III-20-23, MPM-PV 1838, MLP 61-II-20-26, MPM-PV 1902, and humerus MPM-PV 1821[13]), indicating slightly slower bone tissue formation than *Aardonyx* and *Sefapanosaurus*. The non-sauropodiform *Riojasaurus* provides a potentially even stronger demonstration, with a

body mass of around 2230 kg, but a bone tissue type suggesting even slower relative tissue deposition ([11] and see STAR Methods). In contrast, species such as *Saturnalia* (10.6 kg[34]), *Leyesaurus* (body mass unknown, but estimated to be 2.5 m in body length, Apaldetti et al.[35]), *Adeopapposaurus* (39.6 kg[34], *Ngwevu* (approximately 108 kg) and *Coloradisaurus* (381 kg; bipedal body mass equation based on femoral shaft circumference from[36]) are all relatively smaller taxa compared to the more derived Sauropoda. It is possible that these taxa grew more slowly because they were smaller.

Although the innermost LAGs have been destroyed by secondary remodeling, the inner and mid-cortex of *Aardonyx* and *Sefapanosaurus* elements reveals the presence of LAGs even from mid-ontogeny, which differs from the more derived Sauropoda. The distribution of growth marks in *Sefapanosaurus* and *Aardonyx* is also regular with a slight decrease in spacing towards the sub-periosteal surface. This is typical of most dinosaurs, but differs from the basal sauropodomorphs *Plateosaurus*, *Massospondylus* and *Mussaurus*, all of which show extreme developmental plasticity[13,16–18]. This suggests that a decrease in developmental plasticity, towards the more regular growth seen in sauropods, occurred around the base of Sauropodiformes (as seen in *Aardoynyx* and *Sefapanosaurus*).

**Rapid growth preceded gigantism**

The bone tissues of *Aardonyx* and *Sefapanosaurus*, medium-sized sauropodiforms (weighing 1–2 tonnes) from the Triassic/Jurassic boundary interval of South Africa, indicate rapid bone tissue formation and the capacity for rapid growth in these taxa. These taxa are characterized by a highly vascularized rapidly forming woven-parallel complex, with a fibrolamellar complex (in which woven bone dominates) found within the inner and mid-cortex of many specimens. The fibrolamellar cortex was more prevalent in the larger *Sefapanosaurus* than

*Aardonyx*. The presence of highly vascularized, rapidly forming bone tissues with an abundance of woven bone in these taxa shows that, although they did not deposit the same amount of bone as the larger lessemsaurids, they were capable of very rapid growth during the favorable growing season. Interestingly, the highly variable growth seen in the more basal *Mussaurus* suggests that high growth rates had begun to appear, but had yet to become fixed in this taxon[13]. The smaller adult body sizes of *Aardonyx* and *Sefapanosaurus* (compared to lessemsaurids and most sauropods) may have resulted either from the occurrence of a shorter seasonal growth period or from variation in the exact rates of growth and bone tissue formation among taxa with similar bone tissue types[37–39]. The presence of growth marks even during mid-ontogeny sets *Aardonyx* and *Sefapanosaurus* apart from the more derived Eusauropoda, which grew in a sustained manner until late ontogeny. The regular spacing of growth marks suggests that these taxa did not exhibit developmental plasticity, unlike some earlier-diverging sauropodomorphs such as *Plateosaurus*, *Massospondylus* and *Mussaurus*[11,13,16,18]. Taken together, our findings contribute to an emerging picture in which sauropodan growth traits evolved gradually among non-sauropodan sauropodomorphs, and especially in sauropodiforms[5, 11, 14, 40]. Our results show that very rapid bone tissue deposition evolved prior to the development of large body size, and instead of rapid growth and gigantism evolving in concert, high seasonal growth rates, and therefore the potential for annual high growth rates, preceded the evolution of giant body size. Rapid growth was potentially advantageous in the environment of these relatively smaller taxa and was most likely a prerequisite for gigantism in later-branching sauropods.

**Acknowledgments**

Thank you to Sekhomotso Gubuza for her aid in thin sectioning. J.B. is supported by GENUS: DSI-NRF Centre of Excellence in Palaeosciences and the Palaeontological Scientific Trust (PAST). J.B. and J.N.C are supported by the National Research Foundation (GUN 136513 and 118794 respectively).

## Author Contributions

Conceptualization, J.B., J.N.C, and R.B.B.; investigation, J.B., J.N.C, and R.B.J.B; osteohistological analysis, J.B.; writing, J.B., J.N.C, and R.B.J.B.

## Declaration of Interests

The authors declare no competing interests.

## Figure Captions

**Figure 1. Osteohistology of *Sefapanosaurus zatronensis* and *Aardonyx celestae* limb bones.** A, *Sefapanosaurus* BP/1/7445 tibia and B, *Aardonyx* BP/1/5379b ulna showing a woven-parallel complex. C, *Sefapanosaurus* BP/1/7436 radius showing a fibrolamellar complex with abundant woven bone. D, *Sefapanosaurus* BP/1/7435 radius and E, *Sefapanosaurus* BP/1/7445 tibia showing increased dominance of parallel-fibered bone towards the outer cortex. F, *Sefapanosaurus* BP/1/7436 radius showing five growth marks. Arrowheads indicate growth marks. Scale bars A–C 100 µm, D, E, 50 µm, F 500 µm. Abbreviations: PFB, parallel-fibered bone; WB, woven bone. [planned for page width]

**Figure 2. Osteohistology of *Sefapanosaurus zatronensis* and *Aardonyx celestae* limb bones.** A, *Sefapanosaurus* BP/1/7435 radius, B, *Aardonyx* BP/1/5379b ulna, C, *Sefapanosaurus* BP/1/7435 radius and D, *Aardonyx* BP/1/6321 radius showing a woven-parallel complex interrupted by annuli and LAGs. E, *Sefapanosaurus* BP/1/7437 ulna and F, *Aardonyx* BP/1/5379b ulna showing continued growth at the sub-periosteal surface. Arrowheads indicate growth marks. Scale bars A–E 500 µm, F, 100 µm. Abbreviation: WB, woven bone. [planned for page width]

**Figure 3. Line diagrams of the *Sefapanosaurus* (A-G) and *Aardonyx* (H-K) elements in this study.** Red lines represent growth marks. A, humerus BP/1/7434. B, radius BP/1/7436. C, radius BP/1/7435. D, ulna BP/1/7437. E, femur BP/1/7444. F, tibia BP/1/7445. G, BP/1/fibula BP/1/7446. [planned for page width]

**Figure 4. Sauropodomorph phylogenetic tree showing only taxa that have been examined histologically (phylogeny after the most recent studies[30,31].** The general trend is a dominance of parallel-fibered bone in the woven-parallel complex in basal sauropodomorphs, to a woven-parallel complex with narrow zones, and an increase in woven bone, but still with narrow zones in the sauropodiforms *Aardonyx* and *Sefapanosaurus*, to a rapidly forming fibrolamellar complex with wide zones in the Lessemsauridae to sustained rapid growth until late ontogeny in the more derived Eusauropoda. Abbreviations: FLC, fibrolamellar complex, GM, growth marks; PFB, parallel-fibered bone, WB, woven bone, WPC, woven-parallel complex. [planned for page width in portrait]

## STAR Methods

### RESOURCE AVAILABILITY

#### *Lead contact*

Further information and requests for resources or protocol details should be directed to and will be fulfilled by the lead contact, Jennifer Botha (jbotha@nasmus.co.za).

#### *Materials Availability*

The thin sections generated from this study are currently housed at the National Museum, Bloemfontein.

### EXPERIMENTAL MODEL AND SUBJECT DETAILS

#### *Geological Context of Specimens*

*Sefapanosaurus* was found in the *Scalenodontoides* Assemblage Zone of the lower Elliot Formation near the town Zastron, Xhariep District, in the Free State, and is latest Triassic in age[7,41]. The geographic coordinates of the type locality are uncertain, but its stratigraphic position in the lower Elliot Formation is lower than that of *Aardonyx*. The *Aardonyx* type locality, located on the farm Spion Kop in the Thabo Mofutsanyane District of the Free State, is from the overlying *Massospondylus* Assemblage Zone of the upper Elliot Formation and is earliest Jurassic in age[6,42]. The material is housed at the Evolutionary Studies Institute, University of the Witwatersrand, Johannesburg, South Africa (BP). The sample of *Sefapanosaurus* includes a humerus, two radii of different sizes, an ulna, femur, tibia and fibula. The bones pertain to at least four individuals[7]. The *Aardonyx* material includes two radii, an ulna, and a fibula. Radius and ulna BP/1/5379 were tentatively assigned to one individual by[6], however the radius is notably shorter than the ulna, introducing the possibility that they may belong to different individuals.

## QUANTIFICATION AND STATISTICAL ANALYSIS

The vascular density was quantified following the same protocol as[43], where 10 mid-cortical fields of view were used to obtain an average vascular canal area. Although it is well-known that these canals would have included nerves and lymph as well as blood vessels, this quantification provides the maximum possible vascular density within a given region of bone and can be quantitatively compared to other elements or species.

## METHOD DETAILS

### Osteohistology

The thin-sectioning process was conducted at the National Museum, Bloemfontein using the same techniques set out in[44]. All the bones were cast prior to thin sectioning. The samples were embedded in Struers Epofix epoxy resin (Cleveland, OH, USA) inside a vacuum chamber. After setting, the resin blocks were cut into thick sections using a Struers Accutom-100 cutting and grinding machine. The thick sections were then stuck to frosted glass slides using the Struers Epofix resin and then ground to approximately 60 μm in thickness using the Struers Accutom-100. The thin-sections were viewed and photographed using a Nikon Eclipse 50i Polarizing microscope with an attached DS-Fi1 digital camera. Photos were captured using NIS Elements D v. 4.6 (Nikon Corp., Tokyo, Japan). Osteohistological terminology follows that of[8,45]. The distance between growth marks and outer bone circumference was measured in millimeters.

### Body mass estimates

Adult body mass estimates were primarily taken from[14,34], which were both based on the same dataset of limb bone measurements. Mass estimates in those works were based on the estimation equations presented by[46] for quadrupeds (using femoral and humeral shaft

342 circumference), and[36] for bipeds (using femoral shaft circumference). Inference of bipedality
343 or quadrupedality were taken from[14] based on discriminant function analysis of the
344 relationship between humeral and femoral shaft circumferences, in which quadrupeds have
345 proportionally robust forelimbs relative to the hind limb than those of bipeds[14,47]. In cases
346 where it was not possible to infer whether a taxon was bipedal or quadrupedal, as in
347 *Aardonyx* and *Sefapanosaurus*, we present body mass estimates for both bipedal and
348 quadrupedal alternatives. Relevant measurements were not available for adult (or near-adult)
349 individuals in some taxa (e.g. *Lessemsaurus*, *Ingentia*). In those cases, we used mass
350 estimates from other methods, either by imputing the masses of taxa with similar overall
351 skeletal dimensions, or from reasoned suggestions in other literature (e.g.[5]).
352
353 ***Data and code availability***
354 **Section 1: Data**
355 All raw data is available in the STAR Methods and Supplementary Figures or is publicly
356 available in existing publications.
357 **Section2: Code**
358 This paper does not report original code.
359 **Section 3**
360 Any additional information required to reanalyze the data reported in this paper is available
361 from the lead contact upon request.
362
363 **Detailed Osteohistological Descriptions**
364 ***Sefapanosaurus zatronensis***

**Humerus**

Humerus BP/1/7434 is large (circumference 146.81 mm) with what would probably have been an open medullary cavity if not for the large number of broken trabeculae distributed throughout this area (Figure S1A). As these bony trabeculae are mostly broken and floating free of the rest of the bone, it is likely that they formed the peri-medullary region and did not naturally fill the medullary cavity during life. The peri-medullary area contains extensive secondary remodeling with resorption cavities and secondary osteons extending to half way through the cortex. However, although secondary osteons are denser within the innermost cortex, they do not overlap to the extent of forming dense Haversian bone. The compact cortex consists of a highly vascularized woven-parallel complex or WPC (combination of woven and parallel-fibered bone sensu[8,45] with numerous primary osteons (14.77 % vascularization) in a laminar to plexiform arrangement (Figure S1B) with some areas forming a fibrolamellar complex where woven bone dominates. There does not appear to be any decrease in vascularization towards the subperiosteal surface. These characteristics indicate that the bone was growing rapidly. However, the bone tissues are interrupted by four growth marks. Growth marks in the form of annuli or Lines of Arrested Growth indicate temporary decreases (annuli) or cessations (LAGs) in bone growth[10]. In humerus BP/1/7434, the growth marks are in the form of annuli of parallel-fibered bone and are usually associated with LAGs, indicating that growth did not just decrease, but ceased during the unfavorable growing period. There is no External Fundamental System (also known as Outer Circumferential Lamellae) in the form of numerous closely spaced LAGs or an avascular slowly growing region at the subperiosteal surface, indicating that the animal was still growing at the time of death. However, there is a slight decrease in the spacing between the LAGs (Table S1) indicating that the animal was most likely a subadult.

**Radii**

There are two radii. BP/1/7436 (estimated circumference 84.89 mm) is smaller than BP/1/7435 (circumference 113.73 mm) and preserves fewer growth marks, suggesting that it is ontogenetically younger than BP/1/7435 (Figure S1C, SD). The smaller radius is slightly crushed, causing numerous small broken trabeculae to be distributed throughout the medullary cavity (Figure S1C). However, as in the humerus, it is probable that the medullary cavity was mostly open during life and that these trabeculae originate from the peri-medullary area. Resorption cavities and large secondary osteons are common in the inner cortex and extend to the mid-cortex, but dense Haversian bone is absent. Growth marks consist of annuli of parallel-fibered bone associated with five LAGs. There is no marked decrease in the LAG spacing nor vascularization towards the periphery, suggesting that this individual was an early subadult at the time of death. Sharpey's fibers extend into the mid-cortex in several places. The bone clearly exhibits rapidly forming bone tissues in the form of a woven-parallel complex with areas of the inner and mid-cortex being dominated by woven bone such that it can be classified as a fibrolamellar complex. The vascular canal arrangement varies from plexiform to longitudinally-oriented primary osteons (10.47% vascularization).

BP/1/7435 is also slightly crushed, but to a lesser extent than BP/1/7436 (Figure S1D). The medullary cavity and peri-medullary area are similar to BP/1/7436. BP/1/7435 exhibits a typical WPC with a predominantly laminar vascular arrangement (Figure S1E, SF). There are areas that contain a large amount of woven bone (Figure S1G) suggesting the presence of the rapidly forming fibrolamellar complex (12.67% vascularization). There appears to be an increase in parallel-fibered bone in the outer cortex. Eleven LAGs can be seen traversing the cortex, some of which are closely spaced, but there are always several layers of vascular canals between them suggesting that the closely spaced LAGs do not

represent double LAGs (i.e. they do not represent a single season). There is no EFS in this bone, nor is there a general decrease in zone width towards the subperiosteal surface, indicating that this individual was still growing when it died.

**Ulna**

Ulna BP/1/7437 (Figure S1H) is very nicely preserved with a large, clear medullary cavity. The peri-medullary region contains numerous large resorption cavities and secondary osteons. The secondary osteons are dense enough to touch one another, but rarely overlap (forming two generations in a few places). The primary cortex appears midway through the bone and consists of a highly vascularized (11.79% vascularization) WPC with predominately laminar vascular canals, but with longitudinally-oriented primary osteons as well (Figure S1I). Five LAGs are visible. The spacing between LAGs decreases only slightly toward the outer cortex. There is no EFS and no clear decreased vascularization at the subperiosteal surface indicating that the individual was still actively growing at the time of death.

**Femur**

Femur BP/1/7444 (Figure S2A) represents the largest bone in the *Sefapanosaurus* sample (circumference 264.02 mm). Due to the large size of the midshaft, the bone had to be cut into four pieces to fit on four separate slides. It was possible to fit the pieces back into two, but a small section from the middle is missing due to saw destruction. However, the amount of bone missing is only a couple of microns thick and does not limit the description of the osteohistology. The majority of the medullary cavity is open, but there are numerous broken bony trabeculae floating in the outermost parts of the cavity (Figure S2A). There has been some inner crushing and separation of parts of the compact cortex, but bone tissues are

clearly discernable. The bone tissues comprise a highly vascularized WPC (Figure S2B, SC) with predominantly a mixture of laminar and plexiform vascular canals (18.47 % vascularization). It is difficult to accurately count the preserved growth marks as the bone appears to have cracked along many of the LAGs, but at least ten regularly spaced LAGs are preserved. There is no evidence of an EFS nor a decrease in vascularization at the subperiosteal surface, showing that the individual was still actively growing at the time of death. There appears to be less woven bone than the humerus, radii or ulna suggesting a slightly slower growth rate, however the 18.47% vascular density, which is the highest amongst all the *Sefapanosaurus* specimens sampled, suggests that it was still growing rapidly and was in an early subadult stage despite its large size. The bone tissues may appear to have more parallel-fibered bone because there is more laminar bone in this individual where the woven bone becomes sandwiched between the primary osteons as discussed at length by Stein and Prondvai[48] in sauropod dinosaurs.

**Tibia**

Tibia BP/1/7445 is a large bone (177.59 mm circumference) with a thick cortex (Figure S2D). The medullary cavity is clear and medium to large resorption cavities have eroded the perimedullary area. Secondary osteons are abundant in the inner cortex and scatter into the mid-cortex. The bone tissue comprises a highly vascularized (9.15% vascularization) woven-parallel complex (Figure S2E), with a fibrolamellar complex being present in the inner and mid-cortex (Figure S2F). There is a slight increase in the amount of parallel-fibered bone in the outermost cortex. However, the bone remains highly vascularized right up to the subperiosteal surface and varies between laminar and longitudinally-oriented primary osteons. Fourteen growth marks in the form of annuli and LAGs interrupt the bone tissues, with several LAGs forming double LAGs (where there is no vascularization between the

lines). Several LAGs are very closely spaced suggesting that they may have been deposited in a single growing season, but vascular canals separate them, thus the possibility that they represent separate seasons cannot be ruled out. There is no EFS.

**Fibula**

Fibula BP/1/7446 is an asymmetrical bone (Figure S2G) with the cortex being thicker on the medial side. Numerous large cracks are present throughout the bone. The medullary cavity is large and almost completed filled with tiny broken loose bony trabeculae. It is difficult to know whether the medullary cavity would have been partially infilled naturally during life. The inner cortex is similar to the other elements with there being numerous secondary osteons, but not to the extent of forming dense Haversian bone. A woven-parallel complex (Figure S2H) is present throughout the cortex with there being more woven bone in the inner cortex. Vascular arrangements vary between plexiform, laminar and in a few places, longitudinally-oriented primary osteons. Eight growth marks in the form of annuli and LAGs interrupt the cortex at fairly regular intervals. There is no EFS and vascularization (5.1% vascularization) remains constant throughout the cortex. Sharpey's fibers extend as far as the mid-cortex in places.

***Aardonyx celestae***

Yates et al.[6] sectioned a rib and scapula fragment in order to age the specimen in their study. They gave a brief description of a highly vascularized woven-parallel complex interrupted by growth marks, but this is not enough information to obtain a detailed account of the growth patterns of this taxon. Hence, further elements have been examined.

**Radii**

The thick compact cortex of radius BP/1/5379 (circumference 109.61 mm) surrounds an open, clear medullary cavity (Figure S3A). There are no loose, broken trabeculae in the medullary cavity. A few large resorption cavities extend from the peri-medullary area into the mid-cortex in a few places, but are generally restricted to the inner cortex. Secondary osteons are common in the inner cortex, but generally are not abundant enough to touch. They become scattered and sparse in the mid-cortex. The bone comprises a highly vascularized (7.09 % vascularization) network of laminar and longitudinally-oriented primary osteons in a woven-parallel complex, with extensive amounts of woven bone in the inner cortex forming a FLC. Growth marks are present, but are very faint, appearing sometimes as bright lines that can only be seen in cross-polarized light or polarized light with a lambda compensator. Five growth marks in the form of annuli, LAGs or bright lines were observed. The fourth and fifth growth marks are very close together and may represent a single season. The outer growth marks are also closer together compared to the inner ones suggesting an overall decrease in growth. Although the two outermost LAGs are closely spaced, they do not represent an EFS as there is clear bone deposition after these growth marks. Thus, it is likely that BP/1/5379 represents a sub-adult. Sharpey's fibers extend into the outer cortex in a few places, particularly along the medial side of the bone.

Radius BP/1/6321 is similar to radius BP/1/5379a in that the medullary cavity is open (Figure S3B), there are large resorption cavities in the peri-medullary region, becoming smaller as they extend into the innermost cortex and secondary osteons are common in the inner cortex, only rarely being dense enough to touch one another and they become more sparsely distributed in the mid-cortex. The two bones are also similar in their bone tissue types, both exhibiting a well-vascularized woven-parallel complex with a mixture of laminar vascular canals and longitudinally-oriented primary osteons (Figure S3C, SD). There are

patches of FLC in the inner cortex of radius BP/1/6321 where woven bone dominates. However, the bones differ in the number and distribution of growth marks. Lenticular osteocyte lacunae are also more common in BP/1/6321 compared to BP/1/5379a, which contains predominantly globular osteocyte lacunae. BP/1/6321 is slightly smaller in circumference (93.93 mm) than BP/1/5379a, but it exhibits 10 LAGs (the outer two probably representing a double LAG). The LAGs are fairly evenly distributed throughout the cortex. Although the LAGs are relatively closely spaced, there is no EFS at the subperiosteal surface. There is a small patch of radiating vascular canals between the second last and last LAG, which is likely pathological, possibly relating to an injury. Sharpey's fibers extend a small distance into the cortex in places, similar to radius BP/1/5379a.

**Ulna**

Ulna BP/1/5379b contains what would probably have been an open medullary cavity during life (Figure S3E). However, pieces of the peri-medullary region have broken off and are preserved inside the cavity. The peri-medullary area contains numerous resorption cavities and secondary osteons. The secondary osteons appear more abundant than those seen in radius BP/1/5379a, with many of them connecting in the inner cortex. The secondary osteons extend into the mid-cortex. The bone tissue comprises a woven-parallel complex with woven bone being more prominent forming a fibrolamellar complex. Osteocyte lacunae vary from being globular in the woven bone areas to being flattened in the lamellae surrounding the vascular canals or along growth marks. In some areas, thick regions of woven bone separate the primary osteons. The tissues are moderately vascularized (5.28% vascularization) with a predominance of laminar and plexiform vascular canals around most of the bone. However, the arrangement changes to longitudinally-oriented primary osteons in some places and there is an area of radially oriented canals as well. Nine growth marks (notably more than in radius

BP/1/5379a) in the form of LAGs interrupt the cortex at regular intervals. The eighth and ninth LAGs are very closely spaced, but do not represent an EFS as the bone was still growing at the time of death. Sharpey's fibers extend into the mid-cortex on the antero-lateral side of the bone.

**Fibula**

Fibula BP/1/6316 has an asymmetrically distributed cortex with it being thinner on the lateral side (Figure S3F). Broken trabecular fragments are preserved in the medullary cavity bunched up to the thinner cortical area, otherwise the medullary cavity is clear. Resorption cavities are fairly extensive in the inner cortex on the thicker side of the bone. Secondary osteons are common in the inner cortex, but do not form dense Haversian bone. A few can be seen scattered in the mid-cortex. The woven-parallel complex becomes FLC in the inner and parts of the mid-cortex. The vascular canals vary between laminar and longitudinally-oriented primary osteons (Figure S3G, SH). There is an increase in parallel-fibered bone towards the subperiosteal surface. Twelve LAGs were counted traversing the cortex. The last two LAGs form a double LAG. There are also two zones that are wider than the others giving the growth mark distribution a more irregular appearance compared to the other *Aardonyx* elements. There is no EFS. Short Sharpey's fibers extend into the outer cortex in a few places, particularly along the antero-medial and posterior sides of the bone.

**Ontogenetic Reconsiderations**

When comparing the growth patterns of taxa within a given clade, it is important to consider the ontogenetic stage of each specimen examined. The *Aardonyx* and *Sefapanosaurus* data were compared with the osteohistology of other sauropodomorph dinosaurs including the basal *Saturnalia*[49] and *Plateosaurus trossingensis* (previously *P.*

565 *engelhardti*)[16,17], as well as the massopods *Riojasaurus*, *Coloradisaurus*, *Massospondylus*,
566 *Ngwevu*, *Leyesaurus*, *Adeopapposaurus*, the sauropodiformes *Mussaurus* and *Leonerasaurus*,
567 the lessemsaurids *Lessemsaurus*, *Ingentia*, and *Ledumahadi*, as well as the eusauropods
568 *Volkheimeria, Patagosaurus*[5,11,30] and *Isanosaurus*[4]. Although a recent study of the South
569 African lessemsaurid *Antetonitrus ingenipes* indicated possible variation in growth
570 strategies[40], almost all of the material, which were humeri, femora and tibiae, were based on a
571 portion of a bonebed labelled NMQR 1705. Although the holotype of *Antetonitrus*
572 (BP/1/4952) was also examined, no images were shown and a description of the bone tissue
573 was limited to a woven-parallel complex (previously fibrolamellar bone) interrupted by
574 annuli[40], similar to other closely related taxa. The NMQR 1705 elements belong to the well-
575 known Maphutseng dinosaur bonebed from the lower Elliot Formation of Lesotho. Recently
576 de Fabrègues and Allain[50] identified a new species of sauropodomorph from this bonebed,
577 namely *Kholumolumo ellenbergerorum*, indicating the presence of at least two taxa in this
578 quarry. Given that *Antetonitrus* is currently only known from the upper Elliot Formation and
579 that only one unique feature pertaining to the NMQR 1705 *Antetonitrus* limb bones could be
580 identified in the humerus that was thin sectioned (the femur and tibia having no
581 autapomorphies), it is possible that the NMQR 1705 material contains more than one species
582 and thus, the growth patterns of NMQR 1705 may represent multiple taxa.

583 The ontogeny of each specimen examined in the studies listed above is described in
584 detail below, as it has implications for the interpretation of the osteohistology and thus, life
585 history comparisons.

586 The basal sauropodomorph *Saturnalia* was first studied by[49] who reported the
587 presence of fibrolamellar bone (i.e. a woven-parallel complex) in a femur. Two growth marks
588 traversed the cortex, but there was no indication of a decrease in growth towards the
589 subperiosteal surface and an EFS was absent. Cerda et al.[11] reassessed *Saturnalia* and the

590 basal sauropodomorph *Plateosaurus trossingensis* based on more recent personal
591 observations made by Martin Sander, who indicated the predominance of parallel-fibered
592 bone over woven bone in both taxa. Given the presence of two growth marks, but absence of
593 overall decrease in growth rate (e.g. decreased vascularization, narrower zones, EFS etc.), it
594 is likely that the *Saturnalia* specimen was a late juvenile to early subadult at the time of
595 death. The *Plateosaurus* samples represent subadult and late subadult individuals[17] and when
596 the inner cortex is examined, a highly vascularized woven-parallel complex is present with a
597 clear abundance of woven bone (Nicole Klein, pers. comm. 2021).
598 The *Riojasaurus* PVL 3526 specimen examined by[11] contains several closely spaced
599 LAGs at the subperiosteal surface suggesting an older ontogenetic stage (identified in Cerda
600 et al.[11] as an EFS, although there is a region of vascularized tissue that was deposited after
601 these growth marks, thus growth may not have ceased). *Riojasaurus* PVL 3669, which is
602 ontogenetically younger, contains a mixture of woven and parallel-fibered bone[11]. Cerda et
603 al.[11] state that parallel-fibered bone dominates throughout the entire cortex, but it is difficult
604 to confirm this as the osteocyte lacunae appear rarely preserved and can only be seen in
605 images showing the outer cortex of the older PVL 3526 specimen. A comparison with this
606 taxon may have to wait until better preserved material is examined.
607 The massopod *Leyesaurus* specimen in the Cerda et al.[11] study contains at least 13
608 growth marks and represents a relatively old individual, with parallel-fibered bone
609 dominating towards the outer cortex as one would expect in an individual that was nearing
610 adult size. Cerda et al.[11] also mention the dominance of parallel-fibered bone over woven
611 bone (i.e. a woven-parallel complex) in the rest of the cortex. However, the authors also note
612 that the bone tissue features in *Leyesaurus* are identical to those of *Massospondylus*, but the
613 latter taxon shows abundant woven bone at earlier ontogenetic stages (Figure S4). It is likely
614 that the two taxa are similar because they are both adults thus, show similar bone tissues

615 because of ontogenetic stage. Younger individuals of *Massospondylus* show the presence of
616 more woven bone, but the *Leyesaurus* specimen is too remodeled in the inner cortex to assess
617 the primary bone tissues of earlier stages.

618 Cerda et al.[11] noted an increase in parallel-fibered bone in the outer cortex of their
619 *Adeopapposaurus* specimen, which is considered to be 77% of the holotype PVS610.
620 However, the holotype is not considered to be the largest known specimen (D. Pol pers.
621 comm. 2022). This makes femur PVSJ569 a subadult, possibly even a young subadult. There
622 appear to be fewer secondary osteons in the inner cortex obscuring the primary bone tissue
623 and the authors note a predominance of parallel-fibered bone throughout the cortex.

624 *Massospondylus* is portrayed in Cerda et al.[11] as having predominantly parallel-
625 fibered bone. However, as the authors note, the specimen used (BP/1/4934) is one of the
626 ontogenetically oldest *Massospondylus* specimens known (see[18]) and although an EFS is
627 absent, there is a clear decrease in growth rate in the form of decreased spacing between
628 successive growth marks near the subperiosteal surface. The outer cortex consists
629 predominantly of parallel-fibered bone, but when the inner and mid-cortex are examined
630 there is an abundance of woven bone, similar to what has been found in younger
631 *Massospondylus* specimens (e.g. BP/1/4860, 5241, 5108, 4934 ranging from 67% maximum
632 known size to 100% maximum known size, see[18] and Figure S4). The dominant bone tissue is
633 WPC with more woven bone in the inner and mid-cortex of some specimens, and parallel-
634 fibered bone dominating in the mid- and outer cortex of other specimens. The woven bone
635 does not appear to be as abundant as that shown for the lessemsaurids *Lessemsaurus* and
636 *Ingentia*[5].

637 *Ngwevu intloko* is a recently erected, closely related taxon to *Massospondylus*
638 *carinatus* from the Early Jurassic of South Africa[30]. The osteohistology of the humerus and
639 femur were examined and a mixture of woven and parallel-fibered bone was present

640 indicating the presence of WPC, but with substantial amounts of parallel-fibered bone
641 particularly towards the outer cortex ([30] and Figure S4). This observation along with the
642 presence of at least 10 growth marks in the femur and decreased zone width towards the
643 subperiosteal surface suggested that the individual was a late subadult (no EFS was
644 observed). However, the prevalence of more parallel-fibered bone throughout the cortex
645 suggests that the very rapidly forming fibrolamellar complex seen in *Lessemsaurus* and
646 *Ingentia* was absent (except for perhaps very early in ontogeny).
647 The bone tissues of the *Coloradisaurus* specimen are badly preserved and Cerda et
648 al.[11] noted it was difficult to accurately identify the bone tissues. They did, however, note the
649 presence of both woven and parallel-fibered bone, but it is difficult to assess from the images
650 which bone matrix is more prominent. The presence of several growth marks traversing the
651 cortex and absence of decreased vascularization towards the subperiosteal surface suggest a
652 subadult stage for this specimen.
653 The ontogenetic status of *Leonerasaurus* is difficult to assess as the outer cortex of the
654 specimen used in Cerda et al.[11] is absent. However, the authors mention that they considered
655 the individual to be nearly fully grown and the bone tissues were a mix of woven and
656 parallel-fibered bone, indicating the presence of WPC, with parallel-fibered bone dominating
657 throughout the cortex that was preserved.
658 *Mussaurus* was examined by[11,51] and more recently by[52]. *Mussaurus* contains WPC
659 that falls under the fibrolamellar complex during very early ontogeny. The individuals
660 examined by Cerda et al.[11] appear to be late subadults, with MPM-PV 1815 containing more
661 closely spaced growth marks in the outer cortex than specimen MLP 61-III-20-22. However,
662 the more recent study by Pol et al.[52] shows a transition from the fibrolamellar complex to a
663 woven-parallel complex, with increasing amounts of parallel-fibered bone in the second to
664 largest individual. The presence of large amounts of woven bone in the largest individual

665 studied (MLP 61-111-20-22), however, as well as the variable incidence of growth marks[11]
666 indicated that more research was required to fully understand the life history of this taxon.
667 Thus, a very recent study by Cerda et al.[13] examined the humeri, femora and fibulae from 13
668 *Mussaurus* individuals of different sizes. Growth rates and the incidence of growth marks are
669 variable amongst the specimens such that there is little correlation between ontogeny and
670 body size. Some individuals exhibit WPC through to mid-ontogeny, others exhibit a
671 predominance of parallel-fibered bone. The authors provided several reasons for this
672 variability including sexual dimorphism, developmental plasticity and incorrect taxon
673 identification, with the most likely being developmental plasticity[13]. *Mussaurus* is slightly
674 more basal than *Aardonyx* and *Sefapanosaurus*. It is possible that *Mussaurus* had begun to
675 develop inconsistent high growth rates, but this rapid growth had yet to become fixed in this
676 taxon's life history.
677 The Argentinian lessemsaurids *Lessemsaurus sauropoides* (PVL 6580, PVL 4822/64)
678 and *Ingentia prima* (PVSJ 1086) both contain a highly vascularized fibrolamellar complex in
679 the inner most cortices, becoming a WPC in the mid- and outer cortices[5,11]. Despite the
680 *Lessemsaurus* specimens containing four to five LAGs and the *Ingentia* individual eight
681 LAGs, none of the individuals were fully grown (i.e. an EFS is absent). The zones between
682 the LAGs are wide and growth marks are present throughout the cortex in both taxa[5]. The
683 osteohistology from a giant South African lessemsaurid, *Ledumahadi mafube* (BP/1/7120)
684 shows that the mid-cortex comprises WPC and the outer cortex transitions into parallel-
685 fibered bone with an EFS[14]. The growth marks are present in at least the outer third of the
686 cortex. However, the individual represents an almost fully grown adult and the inner cortex is
687 completely remodeled[14]. Thus, we cannot confirm the presence of growth marks throughout
688 the entire cortex as is seen in *Lessemsaurus* and *Ingentia*. Additionally, comparing this
689 individual with the other lessemsaurids is difficult because *Lessemsaurus* and *Ingentia*

represent relatively ontogenetically young individuals (with *Lessemsaurus* PVL 6580 possibly representing a juvenile, see[5]).

Cerda et al.[11] also examined the basal eusauropods, *Patagosaurus* and *Volkheimeria*. The *Patagosaurus* specimen, PVL 4075, did not contain an EFS and exhibited "regularly spaced annuli" with no clear reduction in growth mark spacing towards the outer cortex, although from the images the annuli are relatively closely spaced towards the outer cortex. This suggests a late subadult stage for this specimen. Growth marks are present only in the outer cortex. Woven bone is more prominent compared to the more basal sauropodomorphs.

The specimen representing *Volkheimeria* is relatively small, growth marks are rare (an exact number is not given, but at least two are shown in the images) and restricted to the outer cortex and the bone lacks an EFS. The specimen used, PVL 4077, may represent a relatively young individual as shown by the presence of highly vascularized woven bone at the subperiosteal surface, showing that the individual was still actively growing at the time of death. Thus, it is possible that growth marks appeared during mid-ontogeny, but this cannot be confirmed until further material is examined.

Sander et al.[4] described the osteohistology of *Isanosaurus* from Thailand. Originally considered to be the oldest sauropod, its age is now uncertain and may be anything from Late Triassic to Late Jurassic in age[49]. The bone tissues of the specimen studied consist of the highly vascularized woven-parallel complex, which Sander et al.[4] described as laminar fibrolamellar bone tissue. Growth marks and polish lines are absent suggesting uninterrupted growth until late ontogeny similar to Neosauropoda. However, this characteristic coupled with the lack of Haversian remodeling in the cortex indicates that a relatively young status for this specimen cannot be ruled out[4] and thus, its life history remains uncertain.

715 **References**

716

717 1.Sander, P.M., Christian, A., Clauss, M., Fechner, R., Gee, C.T., Griebeler, E-M., Gunga, H-
718 C., Hummel, J., Mallison, H., Perry, S.F., Preuschoft, H., Rauhut, O.W.M., Remes, K.,
719 Tütken, T., Wings, O., Witzel, U. 2011a. Biology of the sauropod dinosaurs: the evolution of
720 gigantism. Biological Reviews of the Cambridge Philosophical Society 86(1), 117–155.
721 https://doi.org/10.1111/j.1469-185X.2010.00137.x

722

723 2. Carballido, J.L., Pol, D., Otero, A., Cerda, I.A., Salgado, L., Garrido, A.C., Ramezani, J.,
724 Cúneo, N.R., Krause, J.M. 2017. A new giant titanosaur sheds light on body mass evolution
725 among sauropod dinosaurs. Proceedings of the Royal Society B 284, 20171219.
726 http://dx.doi.org/10.1098/rspb.2017.1219.

727

728 3. Sander, P.M., Klein, N., Stein, K., Wings, O. 2011b. Sauropod bone histology and
729 implications for sauropod biology. In: Klein, N., Remes, K., Gee, C.T., Sander, P.M. (Eds.),
730 Biology of the sauropod dinosaurs: understanding the life of giants, Indiana University Press,
731 Bloomington, 276–302.

732

733 4. Sander, P.M., Klein, N., Buffetaut, E., Cuny, G., Suteethorn, V., Le Loeuff, J. 2004.
734 Adaptive radiation in sauropod dinosaurs: Bone histology indicates rapid evolution of giant
735 body size through acceleration. Organisms Diversity and Evolution 4, 165–173.

736

737 5. Apaldetii, C., Martínez, R.N., Cerda, I.A., Pol, D., Alcober, O. 2018. An early trend
738 towards gigantism in Triassic sauropodomorph dinosaurs. Nature Ecology and Evolution
739 2(8), 1227–1232. https://doi.org/10.1038/s41559-018-0599-y

740

741 6. Yates, A.M., Bonnan, M.F., Neveling, J., Chinsamy, A., Blackbeard, M.G. 2010. A new
742 transitional sauropodomorph dinosaur from the Early Jurassic of South Africa and the
743 evolution of sauropod feeding and quadrupedalism. Proceedings of the Royal Society B 277,
744 787–794. https://doi.org/10.1098/rspb.2009.1440

745

746 7. Otero, A., Krupandan, E., Pol, D., Chinsamy, A., Choiniere, J. 2015. A new basal
747 sauropodiform from South Africa and the phylogenetic relationships of basal
748 sauropodomorphs. Zoological Journal of the Linnean Society 174, 589–634.
749 https://doi.org/10.1111/zoj.12247

750

751 8. Buffrénil, V. de, Ricqlès, A.J. de, Zylberberg, L., Padian, K. (Eds). 2021. Skeletal
752 histology and paleohistology, CRC Press, New York.

753

754 9. Francillon-Vieillot, H., Buffrénil, de V., Castanet, J., Geraudie, J., Meunier, F.J., Sire, J.Y.,
755 Zylberberg, L., Ricqlès, de A. 1990. Microstructure and mineralization of vertebrate skeletal
756 tissues. In: Carter J.G. (Ed.), Skeletal Biomineralization: Patterns, Processes and
757 Evolutionary Trends, Van Nestrand Reinhold, New York, 471–548.

758

759 10. Hutton, J.M. 1986. Age determination of living Nile crocodiles from the cortical
760 stratification of bone. Copeia 332–341.

761

762 11. Cerda, I.A., Chinsamy, A., Pol, D., Apaldetti, C., Otero, A., Powell, J.E., Martínez, R.N.
763 2017. Novel insight into the origin of the growth dynamics of sauropod dinosaurs. PLoS
764 ONE 12(6), e0179707. https://doi.org/10.1371/journal.pone.017907

765

766 12. Pol, D., Otero, A., Apaldetti, C., Martínez, R.N. 2021. Triassic sauropodomorph
767 dinosaurs from South America: The origin and diversification of dinosaur dominated
768 herbivorous faunas. Journal of South American Earth Sciences 107, 103145.
769 https://doi.org/10.1016/j.jsames.2020.103145

770

771 13. Cerda, I. A., Pol, D., Otero, A., Chinsamy, A. 2022. Palaeobiology of the early
772 sauropodomorph *Mussaurus patagonicus* inferred from its long bone histology.
773 Palaeontology e12614.

774

775 14. McPhee, B., Benson, R, Botha-Brink, J., Bordy, E., Choiniere, J. 2018. A giant dinosaur
776 from the earliest Jurassic of South Africa and the transition to quadrupedality in early
777 sauropodomorphs. Current Biology 28, 3143–3153.
778 https://doi.org/10.1016/j.cub.2018.07.063

779

780 15. Padian, K., Lamm, E-T. (Eds). 2013. Bone histology of fossil tetrapods: advancing
781 methods, analysis, and interpretation. University of California Press, Berkeley.

782

783 16. Sander, P.M. and Klein, N. 2005. Developmental plasticity in the life history of a
784 prosauropod dinosaur. Science 310, 1800–1802.

785

786 17. Klein, N. and Sander, P.M. 2007. Bone histology and growth of the prosauropod dinosaur
787 *Plateosaurus engelhardti* von Meyer, 1837 from the Norian bonebeds of Trossingen
788 (Germany) and Frick (Switzerland). Special Papers in Palaeontology 77, 169–206.

789

790 18. Chapelle, K.E.J., Botha, J., Choiniere, J.N. 2021. Extreme growth plasticity in the early
791 branching sauropodomorph *Massospondylus carinatus*. Biology Letters 17, 20200843.
792 https://doi.org/10.1098/rsbl.2020.0843.
793
794 19. Ricqlès, A., de, K. Padian, Horner, J.R. 2003. On the bone histology of some Triassic
795 pseudosuchian archosaurs and related taxa. Annales de Paléontologie 89, 67–101.
796
797 20. Botha-Brink, J., Smith, R.M.H. 2011. Osteohistology of the Triassic archosauromorphs
798 *Prolacerta*, *Proterosuchus*, *Euparkeria* and *Erythrosuchus* from the Karoo Basin of South
799 Africa. Journal of Vertebrate Paleontology 31(6), 1238–1254.
800 https://doi.org/10.1080/02724634.2011.621797.
801
802 21. Gower, D.J., R.J. Butler, A.G. Sennikov, J. Hancox, Botha-Brink, J. 2014. A new species
803 of *Garjainia ochev*, 1958 (Diapsida: Archosauriformes: Erythrosuchidae) from the Early
804 Triassic of South Africa. PLoS ONE 9, 11: e111154.
805 https://doi.org/10.1371/journal.pone.0111154.
806
807 22. Hedrick, B.P., Tumarkin-Deratzian, A.R., Dodson, P. 2014. Bone microstructure and
808 relative age of the holotype specimen of the diplodocoid sauropod dinosaur *Suuwassea*
809 *emilieae*. Acta Palaeontologica Polonica 59(2), 292–304.
810
811 23. Woodward, H.N., Freedman Fowler, E.A., Farlow, J.O., Horner, J.R. 2015. *Maiasaura*, a
812 model organism for extinct vertebrate population biology: a large sample statistical
813 assessment of growth dynamics and survivorship. Paleobiology 41(4), 503–527.
814

24. Klein, N. and Sander, P.M. 2008. Ontogenetic stages in the long bone histology of sauropod dinosaurs. Paleobiology 34(2), 247–263.

25. Mitchell, J., Sander, P.M., Stein, K. 2017. Can secondary osteons be used as ontogenetic indicators in sauropods? Extending the histological ontogenetic stages into senescence. Paleobiology. 43, 321–342.

26. Curry, K.A. 1999. Ontogenetic histology of *Apatosaurus* (Dinosauria: Sauropoda): new insights on growth rates and longevity. Journal of Vertebrate Paleontology 19(4), 654–665.

27. Horner, J.R., de Ricqlès, A., Padian, K. 1999. Variation in dinosaur skeletochronology indicators: implications for age assessment and physiology. Paleobiology 25(3), 295–304.

28. Horner, J.R., de Ricqlès, A., Padian, K. 2000. Long bone histology of the hadrosaurid dinosaur *Maiasaura peeblesorum*: growth dynamics and physiology based on an ontogenetic series of skeletal elements. Journal of Vertebrate Paleontology 20(1), 115–129.

29. Werning, S. 2012. The ontogenetic osteohistology of *Tenontosaurus tilletti*. PLoS ONE 7(3), e33539.

30. Chapelle, K.E.J., Barrett, P.M., Botha, J., Choiniere J.N. 2019. *Ngwevu intloko*: a new early sauropodomorph dinosaur from the Lower Jurassic Elliot Formation of South Africa and comments on cranial ontogeny in *Massospondylus carinatus*. PeerJ. https://doi.org/10.7717/peerj.7240

840 31. Rauhut, O.W.M., Holwerda, F.M., Furrer, H. 2020. A derived sauropodiform dinosaur
841 and other sauropodomorph material from the Late Triassic of Canton Schaffhausen,
842 Switzerland. Swiss Journal of Geosciences 113, 8. https://doi.org/10.1186/s00015-020-
843 00360-8.
844
845 32. Apaldetti, C., Pol, D., Ezcurra, M.D., Martínez, R.N. 2021. Sauropodomorph evolution
846 across the Triassic-Jurassic boundary: body size, locomotion, and their influence on
847 morphological disparity. Scientific Reports 11, 22534.
848
849 33. Case, T.J. 1978. Speculations on the growth rate and reproduction of some dinosaurs.
850 Paleobiology, 4, 320–328.
851
852 34. Benson, B.J., Hunt, G., Carrano, M.T., Campione, N. 2018. Cope's Rule and the adaptive
853 landscape of dinosaur body size evolution. Palaeontology 61(1), 13–48.
854
855 35. Apaldetti, C., Martinez, R. N., Alcober, O. A., Pol, D. 2011. A new basal
856 sauropodomorph (Dinosauria: Saurischia) from Quebrada del Barro Formation (Marayes-El
857 Carrizal Basin), Northwestern Argentina. PLoS ONE 6(11), e26964.
858 https://doi.org/10.1371/journal.pone.0026964.
859
860 36. Campione, N.E., Evans, D.C., Brown, C.M., Carrano, M.T. 2014. Body mass estimation
861 in non-avian bipeds using a theoretical conversion to quadruped stylopodial proportions.
862 Methods in Ecology and Evolution, 5(9), 913–923.
863

37. Starck, J.M., Chinsamy, A. 2002. Bone microstructure and developmental plasticity in birds and other dinosaurs. Journal of Morphology. 254, 232–246.

38. Margerie, E.de, Cubo, J., Castanet, J. 2002. Bone typology and growth rate: testing and quantifying 'Amprino's rule' in the mallard (*Anas platyrhynchos*). Comptes Rendus Biologies 325, 221–230.

39. Margerie, E.de, Robin, J.-P., Verrier, D. Cubo, J., Groscolas, R., Castanet, J. 2004. Assessing a relationship between bone microstructure and growth rate: a fluorescent labelling study in the king penguin chick (*Aptenodytes patagonicus*). The Journal of Experimental Biology 207, 869–879.

40. Krupandan, E., Chinsamy-Turan, A., Pol, D. 2018. The long bone histology of the sauropodomorph, *Antetonitrus ingenipes*. The Anatomical Record 301, 1506–1518.

41. Viglietti, P.A., McPhee, B.W., Bordy, E.M., Sciscio, L., Barrett, P.M., Benson, R.B.J., Wills, S., Tolchard, F., Choiniere, J.N. 2020a. Biostratigraphy of the *Scalenodontoides* Assemblage Zone (Stormberg Group, Karoo Supergroup), South Africa. In: Smith, R.M.H. (Ed.) Karoo biostratigraphy. Special Issue. South African Journal of Geology 123(2), 239–248. https://doi.org/10.25131/sajg.123.0017

42. Viglietti, P.A., McPhee, B.W., Bordy, E.M., Sciscio, L., Barrett, P.M., Benson, R.B.J., Wills, S., Chapelle, K.E.J., Dollman, K.N., Medkazi, C., Choiniere, J.N. 2020b. Biostratigraphy of the *Massospondylus* Assemblage Zone (Stormberg Group, Karoo

888 Supergroup), South Africa. In: Smith, R.M.H. (Ed.) Karoo biostratigraphy. Special Issue.
889 South African Journal of Geology 123(2), 249–262. https://doi.org/10.25131/sajg.123.0018
890
891 43. Botha, J. 2020. The paleobiology and paleoecology of South African *Lystrosaurus*. PeerJ,
892 8, e10408. https://doi.org/10.7717/peerj.10408.
893
894 44. Botha-Brink, J., Soares, M.B., Martinelli, A.G. 2018. Osteohistology of Late Triassic
895 prozostrodontian cynodonts from Brazil. PeerJ 6:e5029. https://doi.org.10.7717/peerj.5029.
896
897 45. Prondvai, E., Stein, K.H., Ricqlès, A. de., Cubo, J. 2014. Development-based revision of
898 bone tissue classification: the importance of semantics for science. Biological Journal of the
899 Linnean Society, 112, 799–816.
900
901 46. Campione, N.E., Evans, D.C. 2012. A universal scaling relationship between body mass
902 and proximal limb bone dimensions in quadrupedal terrestrial tetrapods. BMC Biology 10, 1–
903 22.
904
905 47. Chapelle, K.E.J., Benson, R.B.J., Stiegler, J., Otero, A., Zhao, Q., Choiniere, J.N. 2020. A
906 quantitative method for inferring locomotory shifts in amniotes during ontogeny, its
907 application to dinosaurs and its bearing on the evolution of posture. Palaeontology 63, 229–
908 242.
909
910 48. Stein, K. and Prondvai, E. 2014. Rethinking the nature of fibrolamellar bone: an
911 integrative biological revision of sauropod plexiform bone formation. Biological Reviews of
912 the Cambridge Philosophical Society 89, 24–47. https://doi.org/10.1111/brv/12041

913

914 49. Stein, K.H.W. 2010. Long bone histology of basalmost and derived Sauropodomorpha:
915 the convergence of fibrolamellar bone and the evolution of gigantism and nanism. PhD
916 dissertation, University of Bonn, Germany, 213pp.

917

918 50. Fabrègues de, C.P., Allain, R. 2020. *Kholumolumo ellenbergerorum*, gen. et sp. nov., a
919 new early sauropodomorph from the lower Elliot Formation (Upper Triassic) of Maphutseng,
920 Lesotho. Journal of Vertebrate Paleontology 39(6), e1732996.
921 https://doi.org/10.1080/02724634.2019.1732996

922

923 51. Cerda, I.A., Pol, D., Chinsamy, A. 2014. Osteohistological insight into the early stages of
924 growth in *Mussaurus patagonicus* (Dinosauria, Sauropodomorpha). Historical Biology 26(1),
925 110–121. http://dx.doi.org/10.1080/08912963.2012.763119

926

927 52. Pol, D., Mancuso, A.C., Smith, R.M.H., Marsicano, C.A., Ramezani, J., Cerda, I.A.,
928 Otero, A., Fernandez, V. 2021. Earliest evidence of herd-living and age segregation amongst
929 dinosaurs. Scientific Reports 11, 20023. https://doi.org/10.1038/s41598-021-99176-1

930

## KEY RESOURCES TABLE

| REAGENT or RESOURCE | SOURCE | IDENTIFIER |
|---|---|---|
| Antibodies | | |
| | | |
| | | |
| | | |
| | | |
| | | |
| Bacterial and virus strains | | |
| | | |
| | | |
| | | |
| | | |
| | | |
| Biological samples | | |
| *Sefapanosaurus zatronensis* osteohistological thin sections | Evolutionary Studies Institute, University of the Witwatersrand | Cat#BP/1/7434; 7436; 7435; 7437; 7444; 7445; 7446, available in www.morphosource.org/projects/000448881 |
| *Aardonyx celestae* osteohistological thin sections | Evolutionary Studies Institute, University of the Witwatersrand | Cat#BP/1/5379a; 6321; 5379b; 6316, available in www.morphosource.org/projects/000448881 |
| Chemicals, peptides, and recombinant proteins | | |

| | | |
|---|---|---|
| | | |
| | | |
| | | |
| | | |
| | | |
| Critical commercial assays | | |
| | | |
| | | |
| | | |
| | | |
| | | |
| Deposited data | | |
| Analyzed data | This paper | https://doi.org/10.17605/OSF.IO/VP435 |
| | | |
| | | |
| | | |
| | | |
| Experimental models: Cell lines | | |
| | | |
| | | |
| | | |
| | | |

| | | |
|---|---|---|
| | | |
| Experimental models: Organisms/strains | | |
| | | |
| | | |
| | | |
| | | |
| | | |
| | | |
| Oligonucleotides | | |
| | | |
| | | |
| | | |
| | | |
| | | |
| Recombinant DNA | | |
| | | |
| | | |
| | | |
| | | |
| | | |
| Software and algorithms | | |
| | | |
| | | |

| | | |
|---|---|---|
| | | |
| | | |
| | | |
| Other | | |
| | | |
| | | |
| | | |
| | | |
| | | |

Figure

Click here to access/download;Figure;Figure 1.tif

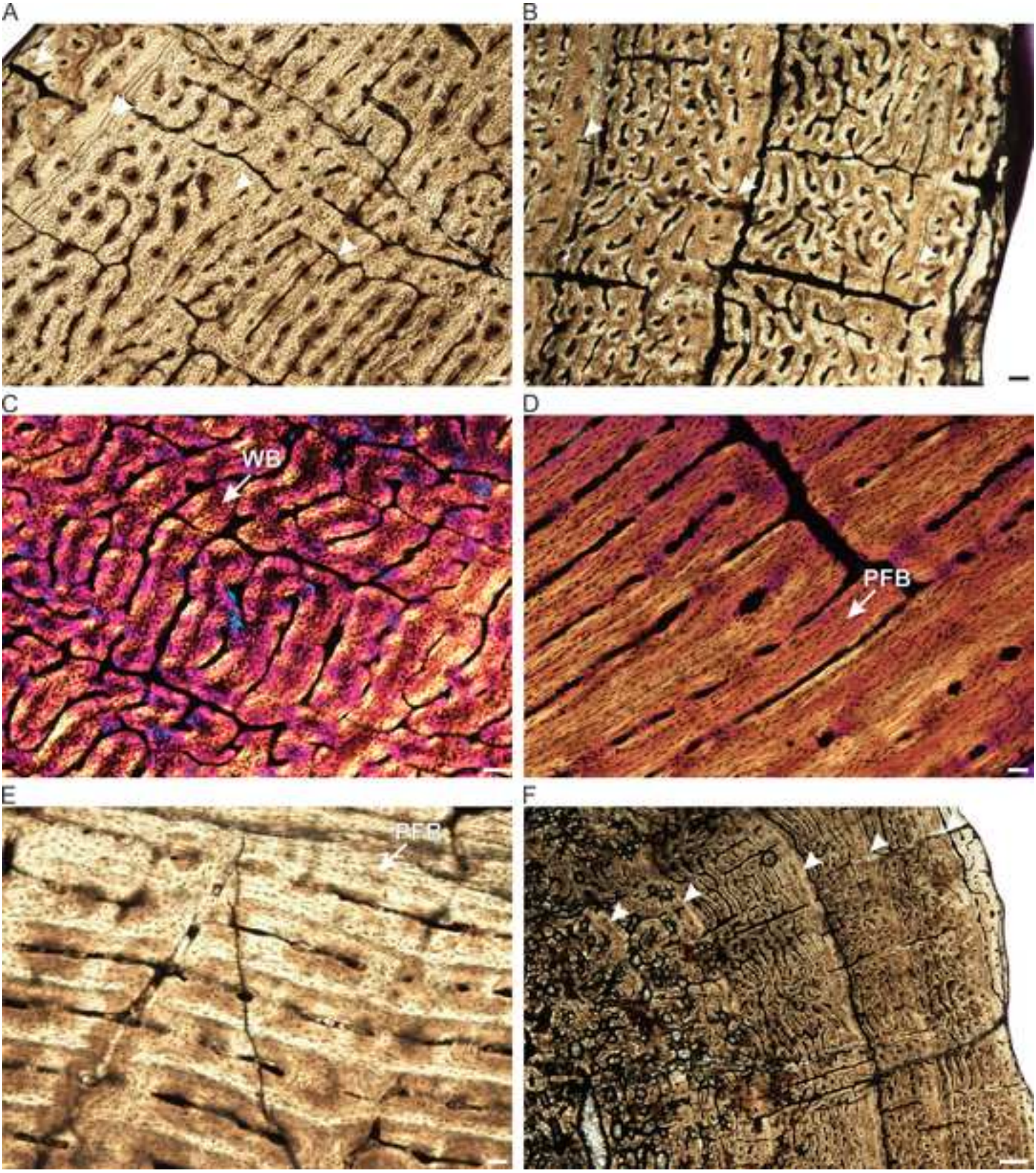

Figure



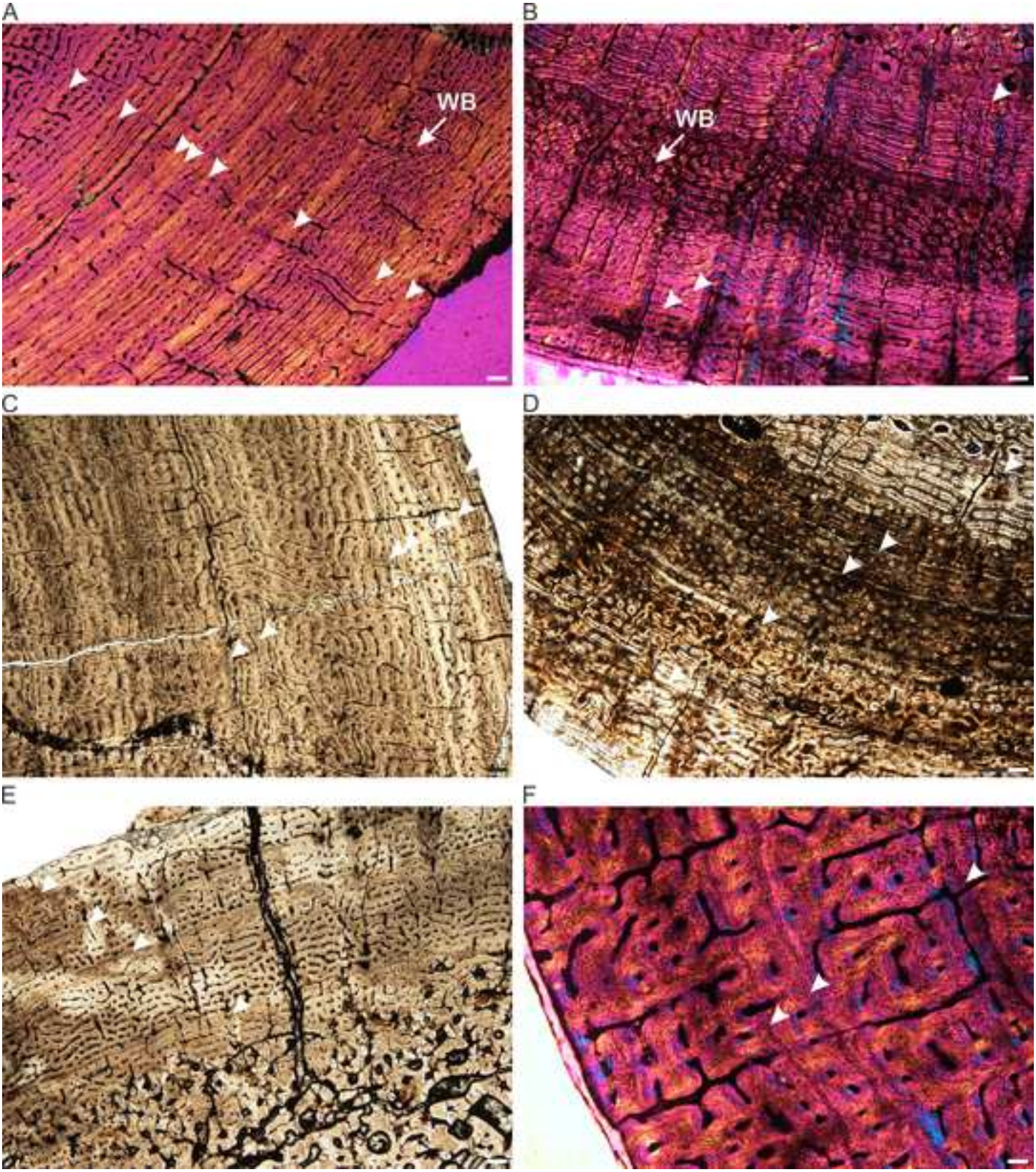

Figure

Click here to access/download;Figure;Figure 3.tif

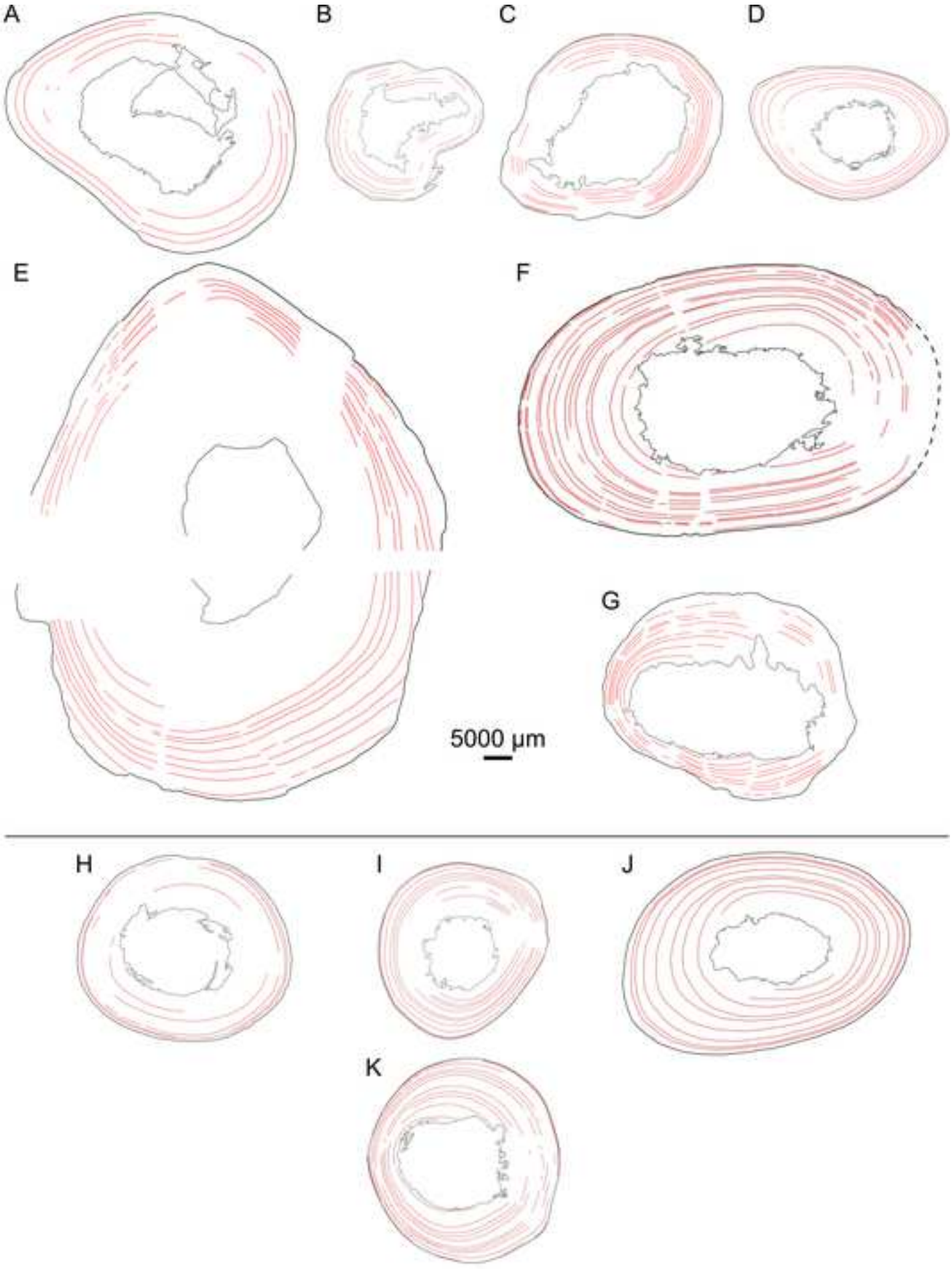

Figure

Click here to access/download;Figure;Figure 4.tif

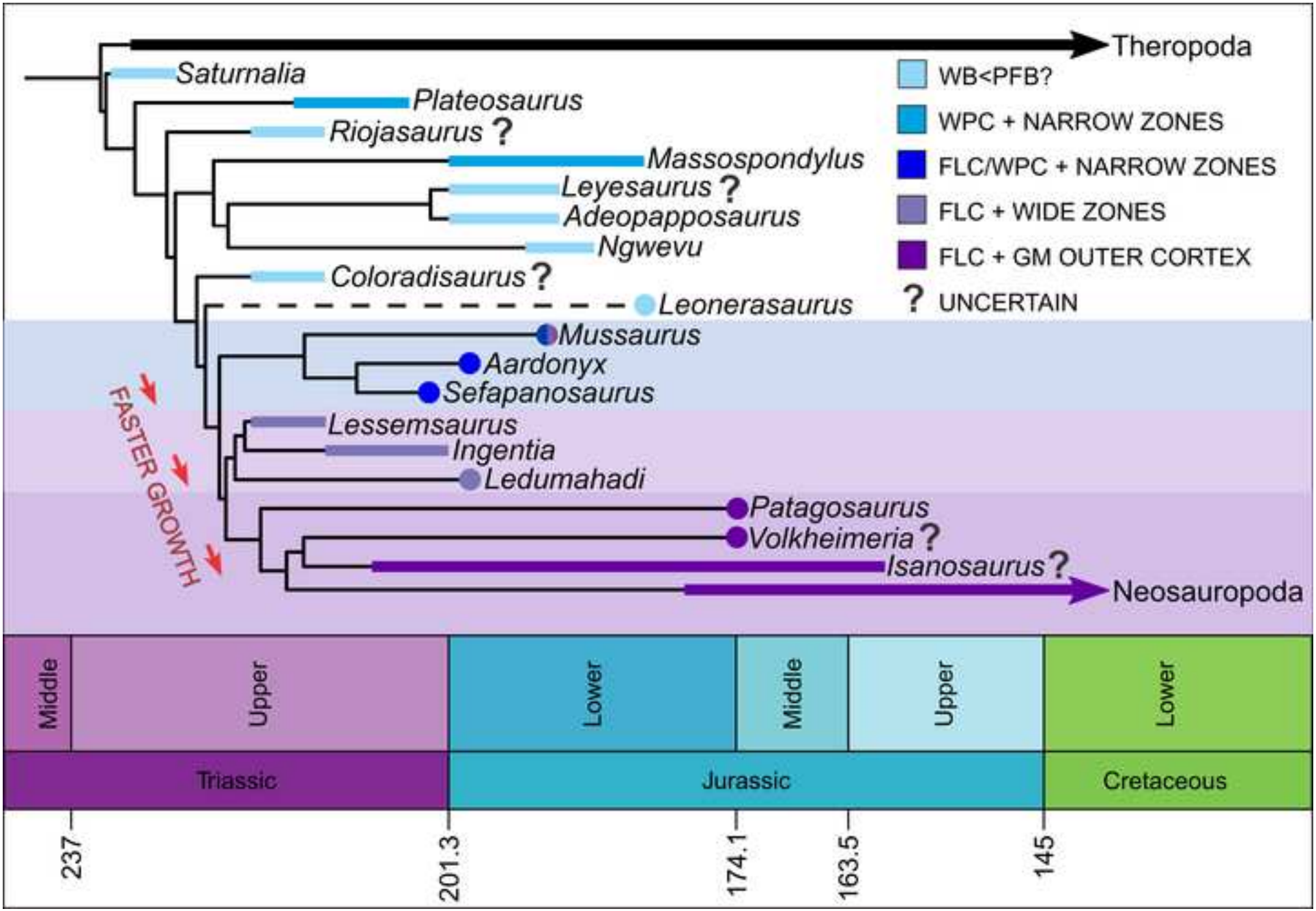

## Detailed Osteohistological Descriptions

### *Sefapanosaurus zatronensis*

### Humerus

Humerus BP/1/7434 is large (circumference 146.81 mm) with what would probably have been an open medullary cavity if not for the large number of broken trabeculae distributed throughout this area (Figure S1A). As these bony trabeculae are mostly broken and floating free of the rest of the bone, it is likely that they formed the peri-medullary region and did not naturally fill the medullary cavity during life. The peri-medullary area contains extensive secondary remodeling with resorption cavities and secondary osteons extending to half way through the cortex. However, although secondary osteons are denser within the innermost cortex, they do not overlap to the extent of forming dense Haversian bone. The compact cortex consists of a highly vascularized woven-parallel complex or WPC (combination of woven and parallel-fibered bone sensu[S1,S2] with numerous primary osteons (14.77 % vascularization) in a laminar to plexiform arrangement (Figure S1B) with some areas forming a fibrolamellar complex where woven bone dominates. There does not appear to be any decrease in vascularization towards the subperiosteal surface. These characteristics indicate that the bone was growing rapidly. However, the bone tissues are interrupted by four growth marks. Growth marks in the form of annuli or Lines of Arrested Growth indicate temporary decreases (annuli) or cessations (LAGs) in bone growth[S3]. In humerus BP/1/7434, the growth marks are in the form of annuli of parallel-fibered bone and are usually associated with LAGs, indicating that growth did not just decrease, but ceased during the unfavorable growing period. There is no External Fundamental System (also known as Outer Circumferential Lamellae) in the form of numerous closely spaced LAGs or an avascular slowly growing region at the subperiosteal surface, indicating that the animal was still

growing at the time of death. However, there is a slight decrease in the spacing between the LAGs (Table S1) indicating that the animal was most likely a subadult.

**Radii**

There are two radii. BP/1/7436 (estimated circumference 84.89 mm) is smaller than BP/1/7435 (circumference 113.73 mm) and preserves fewer growth marks, suggesting that it is ontogenetically younger than BP/1/7435 (Figure S1C, SD). The smaller radius is slightly crushed, causing numerous small broken trabeculae to be distributed throughout the medullary cavity (Figure S1C). However, as in the humerus, it is probable that the medullary cavity was mostly open during life and that these trabeculae originate from the peri-medullary area. Resorption cavities and large secondary osteons are common in the inner cortex and extend to the mid-cortex, but dense Haversian bone is absent. Growth marks consist of annuli of parallel-fibered bone associated with five LAGs. There is no marked decrease in the LAG spacing nor vascularization towards the periphery, suggesting that this individual was an early subadult at the time of death. Sharpey's fibers extend into the mid-cortex in several places. The bone clearly exhibits rapidly forming bone tissues in the form of a woven-parallel complex with areas of the inner and mid-cortex being dominated by woven bone such that it can be classified as a fibrolamellar complex. The vascular canal arrangement varies from plexiform to longitudinally-oriented primary osteons (10.47% vascularization).

BP/1/7435 is also slightly crushed, but to a lesser extent than BP/1/7436 (Figure S1D). The medullary cavity and peri-medullary area are similar to BP/1/7436. BP/1/7435 exhibits a typical WPC with a predominantly laminar vascular arrangement (Figure S1E, SF). There are areas that contain a large amount of woven bone (Figure S1G) suggesting the presence of the rapidly forming fibrolamellar complex (12.67% vascularization). There

appears to be an increase in parallel-fibered bone in the outer cortex. Eleven LAGs can be seen traversing the cortex, some of which are closely spaced, but there are always several layers of vascular canals between them suggesting that the closely spaced LAGs do not represent double LAGs (i.e. they do not represent a single season). There is no EFS in this bone, nor is there a general decrease in zone width towards the subperiosteal surface, indicating that this individual was still growing when it died.

**Ulna**

Ulna BP/1/7437 (Figure S1H) is very nicely preserved with a large, clear medullary cavity. The peri-medullary region contains numerous large resorption cavities and secondary osteons. The secondary osteons are dense enough to touch one another, but rarely overlap (forming two generations in a few places). The primary cortex appears midway through the bone and consists of a highly vascularized (11.79% vascularization) WPC with predominately laminar vascular canals, but with longitudinally-oriented primary osteons as well (Figure S1I). Five LAGs are visible. The spacing between LAGs decreases only slightly toward the outer cortex. There is no EFS and no clear decreased vascularization at the subperiosteal surface indicating that the individual was still actively growing at the time of death.

**Femur**

Femur BP/1/7444 (Figure S2A) represents the largest bone in the *Sefapanosaurus* sample (circumference 264.02 mm). Due to the large size of the midshaft, the bone had to be cut into four pieces to fit on four separate slides. It was possible to fit the pieces back into two, but a small section from the middle is missing due to saw destruction. However, the amount of bone missing is only a couple of microns thick and does not limit the description of the

osteohistology. The majority of the medullary cavity is open, but there are numerous broken bony trabeculae floating in the outermost parts of the cavity (Figure S2A). There has been some inner crushing and separation of parts of the compact cortex, but bone tissues are clearly discernable. The bone tissues comprise a highly vascularized WPC (Figure S2B, SC) with predominantly a mixture of laminar and plexiform vascular canals (18.47 % vascularization). It is difficult to accurately count the preserved growth marks as the bone appears to have cracked along many of the LAGs, but at least ten regularly spaced LAGs are preserved. There is no evidence of an EFS nor a decrease in vascularization at the subperiosteal surface, showing that the individual was still actively growing at the time of death. There appears to be less woven bone than the humerus, radii or ulna suggesting a slightly slower growth rate, however the 18.47% vascular density, which is the highest amongst all the *Sefapanosaurus* specimens sampled, suggests that it was still growing rapidly and was in an early subadult stage despite its large size. The bone tissues may appear to have more parallel-fibered bone because there is more laminar bone in this individual where the woven bone becomes sandwiched between the primary osteons as discussed at length by Stein and Prondvai[4] in sauropod dinosaurs.

**Tibia**

Tibia BP/1/7445 is a large bone (177.59 mm circumference) with a thick cortex (Figure S2D). The medullary cavity is clear and medium to large resorption cavities have eroded the perimedullary area. Secondary osteons are abundant in the inner cortex and scatter into the mid-cortex. The bone tissue comprises a highly vascularized (9.15% vascularization) woven-parallel complex (Figure S2E), with a fibrolamellar complex being present in the inner and mid-cortex (Figure S2F). There is a slight increase in the amount of parallel-fibered bone in the outermost cortex. However, the bone remains highly vascularized right up to the

subperiosteal surface and varies between laminar and longitudinally-oriented primary osteons. Fourteen growth marks in the form of annuli and LAGs interrupt the bone tissues, with several LAGs forming double LAGs (where there is no vascularization between the lines). Several LAGs are very closely spaced suggesting that they may have been deposited in a single growing season, but vascular canals separate them, thus the possibility that they represent separate seasons cannot be ruled out. There is no EFS.

**Fibula**

Fibula BP/1/7446 is an asymmetrical bone (Figure S2G) with the cortex being thicker on the medial side. Numerous large cracks are present throughout the bone. The medullary cavity is large and almost completed filled with tiny broken loose bony trabeculae. It is difficult to know whether the medullary cavity would have been partially infilled naturally during life. The inner cortex is similar to the other elements with there being numerous secondary osteons, but not to the extent of forming dense Haversian bone. A woven-parallel complex (Figure S2H) is present throughout the cortex with there being more woven bone in the inner cortex. Vascular arrangements vary between plexiform, laminar and in a few places, longitudinally-oriented primary osteons. Eight growth marks in the form of annuli and LAGs interrupt the cortex at fairly regular intervals. There is no EFS and vascularization (5.1% vascularization) remains constant throughout the cortex. Sharpey's fibers extend as far as the mid-cortex in places.

***Aardonyx celestae***

Yates et al.[S5] sectioned a rib and scapula fragment in order to age the specimen in their study. They gave a brief description of a highly vascularized woven-parallel complex interrupted by

growth marks, but this is not enough information to obtain a detailed account of the growth patterns of this taxon. Hence, further elements have been examined.

**Radii**

The thick compact cortex of radius BP/1/5379 (circumference 109.61 mm) surrounds an open, clear medullary cavity (Figure S3A). There are no loose, broken trabeculae in the medullary cavity. A few large resorption cavities extend from the peri-medullary area into the mid-cortex in a few places, but are generally restricted to the inner cortex. Secondary osteons are common in the inner cortex, but generally are not abundant enough to touch. They become scattered and sparse in the mid-cortex. The bone comprises a highly vascularized (7.09 % vascularization) network of laminar and longitudinally-oriented primary osteons in a woven-parallel complex, with extensive amounts of woven bone in the inner cortex forming a FLC. Growth marks are present, but are very faint, appearing sometimes as bright lines that can only be seen in cross-polarized light or polarized light with a lambda compensator. Five growth marks in the form of annuli, LAGs or bright lines were observed. The fourth and fifth growth marks are very close together and may represent a single season. The outer growth marks are also closer together compared to the inner ones suggesting an overall decrease in growth. Although the two outermost LAGs are closely spaced, they do not represent an EFS as there is clear bone deposition after these growth marks. Thus, it is likely that BP/1/5379 represents a sub-adult. Sharpey's fibers extend into the outer cortex in a few places, particularly along the medial side of the bone.

Radius BP/1/6321 is similar to radius BP/1/5379a in that the medullary cavity is open (Figure S3B), there are large resorption cavities in the peri-medullary region, becoming smaller as they extend into the innermost cortex and secondary osteons are common in the inner cortex, only rarely being dense enough to touch one another and they become more

sparsely distributed in the mid-cortex. The two bones are also similar in their bone tissue types, both exhibiting a well-vascularized woven-parallel complex with a mixture of laminar vascular canals and longitudinally-oriented primary osteons (Figure S3C, SD). There are patches of FLC in the inner cortex of radius BP/1/6321 where woven bone dominates. However, the bones differ in the number and distribution of growth marks. Lenticular osteocyte lacunae are also more common in BP/1/6321 compared to BP/1/5379a, which contains predominantly globular osteocyte lacunae. BP/1/6321 is slightly smaller in circumference (93.93 mm) than BP/1/5379a, but it exhibits 10 LAGs (the outer two probably representing a double LAG). The LAGs are fairly evenly distributed throughout the cortex. Although the LAGs are relatively closely spaced, there is no EFS at the subperiosteal surface. There is a small patch of radiating vascular canals between the second last and last LAG, which is likely pathological, possibly relating to an injury. Sharpey's fibers extend a small distance into the cortex in places, similar to radius BP/1/5379a.

**Ulna**

Ulna BP/1/5379b contains what would probably have been an open medullary cavity during life (Figure S3E). However, pieces of the peri-medullary region have broken off and are preserved inside the cavity. The peri-medullary area contains numerous resorption cavities and secondary osteons. The secondary osteons appear more abundant than those seen in radius BP/1/5379a, with many of them connecting in the inner cortex. The secondary osteons extend into the mid-cortex. The bone tissue comprises a woven-parallel complex with woven bone being more prominent forming a fibrolamellar complex. Osteocyte lacunae vary from being globular in the woven bone areas to being flattened in the lamellae surrounding the vascular canals or along growth marks. In some areas, thick regions of woven bone separate the primary osteons. The tissues are moderately vascularized (5.28% vascularization) with a

predominance of laminar and plexiform vascular canals around most of the bone. However, the arrangement changes to longitudinally-oriented primary osteons in some places and there is an area of radially oriented canals as well. Nine growth marks (notably more than in radius BP/1/5379a) in the form of LAGs interrupt the cortex at regular intervals. The eighth and ninth LAGs are very closely spaced, but do not represent an EFS as the bone was still growing at the time of death. Sharpey's fibers extend into the mid-cortex on the antero-lateral side of the bone.

**Fibula**

Fibula BP/1/6316 has an asymmetrically distributed cortex with it being thinner on the lateral side (Figure S3F). Broken trabecular fragments are preserved in the medullary cavity bunched up to the thinner cortical area, otherwise the medullary cavity is clear. Resorption cavities are fairly extensive in the inner cortex on the thicker side of the bone. Secondary osteons are common in the inner cortex, but do not form dense Haversian bone. A few can be seen scattered in the mid-cortex. The woven-parallel complex becomes FLC in the inner and parts of the mid-cortex. The vascular canals vary between laminar and longitudinally-oriented primary osteons (Figure S3G, SH). There is an increase in parallel-fibered bone towards the subperiosteal surface. Twelve LAGs were counted traversing the cortex. The last two LAGs form a double LAG. There are also two zones that are wider than the others giving the growth mark distribution a more irregular appearance compared to the other *Aardonyx* elements. There is no EFS. Short Sharpey's fibers extend into the outer cortex in a few places, particularly along the antero-medial and posterior sides of the bone.

**Ontogenetic Reconsiderations**

When comparing the growth patterns of taxa within a given clade, it is important to consider the ontogenetic stage of each specimen examined. The *Aardonyx* and *Sefapanosaurus* data were compared with the osteohistology of other sauropodomorph dinosaurs including the basal *Saturnalia*[6] and *Plateosaurus trossingensis* (previously *P. engelhardti*)[S7,S8], as well as the massopods *Riojasaurus*, *Coloradisaurus*, *Massospondylus*, *Ngwevu*, *Leyesaurus*, *Adeopapposaurus*, the sauropodiformes *Mussaurus* and *Leonerasaurus*, the lessemsaurids *Lessemsaurus*, *Ingentia*, and *Ledumahadi*, as well as the eusauropods *Volkheimeria, Patagosaurus*[S9,S10,S11] and *Isanosaurus*[S12]. Although a recent study of the South African lessemsaurid *Antetonitrus ingenipes* indicated possible variation in growth strategies[S13], almost all of the material, which were humeri, femora and tibiae, were based on a portion of a bonebed labelled NMQR 1705. Although the holotype of *Antetonitrus* (BP/1/4952) was also examined, no images were shown and a description of the bone tissue was limited to a woven-parallel complex (previously fibrolamellar bone) interrupted by annuli[S13], similar to other closely related taxa. The NMQR 1705 elements belong to the well-known Maphutseng dinosaur bonebed from the lower Elliot Formation of Lesotho. Recently de Fabrègues and Allain[S14] identified a new species of sauropodomorph from this bonebed, namely *Kholumolumo ellenbergerorum*, indicating the presence of at least two taxa in this quarry. Given that *Antetonitrus* is currently only known from the upper Elliot Formation and that only one unique feature pertaining to the NMQR 1705 *Antetonitrus* limb bones could be identified in the humerus that was thin sectioned (the femur and tibia having no autapomorphies), it is possible that the NMQR 1705 material contains more than one species and thus, the growth patterns of NMQR 1705 may represent multiple taxa.

The ontogeny of each specimen examined in the studies listed above is described in detail below, as it has implications for the interpretation of the osteohistology and thus, life history comparisons.

The basal sauropodomorph *Saturnalia* was first studied by[S6] who reported the presence of fibrolamellar bone (i.e. a woven-parallel complex) in a femur. Two growth marks traversed the cortex, but there was no indication of a decrease in growth towards the subperiosteal surface and an EFS was absent. Cerda et al.[S10] reassessed *Saturnalia* and the basal sauropodomorph *Plateosaurus trossingensis* based on more recent personal observations made by Martin Sander, who indicated the predominance of parallel-fibered bone over woven bone in both taxa. Given the presence of two growth marks, but absence of overall decrease in growth rate (e.g. decreased vascularization, narrower zones, EFS etc.), it is likely that the *Saturnalia* specimen was a late juvenile to early subadult at the time of death. The *Plateosaurus* samples represent subadult and late subadult individuals[S8] and when the inner cortex is examined, a highly vascularized woven-parallel complex is present with a clear abundance of woven bone (Nicole Klein, pers. comm. 2021).

The *Riojasaurus* PVL 3526 specimen examined by[S10] contains several closely spaced LAGs at the subperiosteal surface suggesting an older ontogenetic stage (identified in Cerda et al.[S10] as an EFS, although there is a region of vascularized tissue that was deposited after these growth marks, thus growth may not have ceased). *Riojasaurus* PVL 3669, which is ontogenetically younger, contains a mixture of woven and parallel-fibered bone[S10]. Cerda et al.[S10] state that parallel-fibered bone dominates throughout the entire cortex, but it is difficult to confirm this as the osteocyte lacunae appear rarely preserved and can only be seen in images showing the outer cortex of the older PVL 3526 specimen. A comparison with this taxon may have to wait until better preserved material is examined.

The massopod *Leyesaurus* specimen in the Cerda et al.[S10] study contains at least 13 growth marks and represents a relatively old individual, with parallel-fibered bone dominating towards the outer cortex as one would expect in an individual that was nearing adult size. Cerda et al.[S10] also mention the dominance of parallel-fibered bone over woven

bone (i.e. a woven-parallel complex) in the rest of the cortex. However, the authors also note that the bone tissue features in *Leyesaurus* are identical to those of *Massospondylus*, but the latter taxon shows abundant woven bone at earlier ontogenetic stages (Figure S4). It is likely that the two taxa are similar because they are both adults thus, show similar bone tissues because of ontogenetic stage. Younger individuals of *Massospondylus* show the presence of more woven bone, but the *Leyesaurus* specimen is too remodeled in the inner cortex to assess the primary bone tissues of earlier stages.

Cerda et al.[S10] noted an increase in parallel-fibered bone in the outer cortex of their *Adeopapposaurus* specimen, which is considered to be 77% of the holotype PVS610. However, the holotype is not considered to be the largest known specimen (D. Pol pers. comm. 2022). This makes femur PVSJ569 a subadult, possibly even a young subadult. There appear to be fewer secondary osteons in the inner cortex obscuring the primary bone tissue and the authors note a predominance of parallel-fibered bone throughout the cortex.

*Massospondylus* is portrayed in Cerda et al.[S10] as having predominantly parallel-fibered bone. However, as the authors note, the specimen used (BP/1/4934) is one of the ontogenetically oldest *Massospondylus* specimens known (see[15]) and although an EFS is absent, there is a clear decrease in growth rate in the form of decreased spacing between successive growth marks near the subperiosteal surface. The outer cortex consists predominantly of parallel-fibered bone, but when the inner and mid-cortex are examined there is an abundance of woven bone, similar to what has been found in younger *Massospondylus* specimens (e.g. BP/1/4860, 5241, 5108, 4934 ranging from 67% maximum known size to 100% maximum known size, see[15] and Figure S4). The dominant bone tissue is WPC with more woven bone in the inner and mid-cortex of some specimens, and parallel-fibered bone dominating in the mid- and outer cortex of other specimens. The woven bone

does not appear to be as abundant as that shown for the lessemsaurids *Lessemsaurus* and *Ingentia*[S9].

*Ngwevu intloko* is a recently erected, closely related taxon to *Massospondylus carinatus* from the Early Jurassic of South Africa[S11]. The osteohistology of the humerus and femur were examined and a mixture of woven and parallel-fibered bone was present indicating the presence of WPC, but with substantial amounts of parallel-fibered bone particularly towards the outer cortex ([S11] and Figure S4). This observation along with the presence of at least 10 growth marks in the femur and decreased zone width towards the subperiosteal surface suggested that the individual was a late subadult (no EFS was observed). However, the prevalence of more parallel-fibered bone throughout the cortex suggests that the very rapidly forming fibrolamellar complex seen in *Lessemsaurus* and *Ingentia* was absent (except for perhaps very early in ontogeny).

The bone tissues of the *Coloradisaurus* specimen are badly preserved and Cerda et al.[S10] noted it was difficult to accurately identify the bone tissues. They did, however, note the presence of both woven and parallel-fibered bone, but it is difficult to assess from the images which bone matrix is more prominent. The presence of several growth marks traversing the cortex and absence of decreased vascularization towards the subperiosteal surface suggest a subadult stage for this specimen.

The ontogenetic status of *Leonerasaurus* is difficult to assess as the outer cortex of the specimen used in Cerda et al.[S10] is absent. However, the authors mention that they considered the individual to be nearly fully grown and the bone tissues were a mix of woven and parallel-fibered bone, indicating the presence of WPC, with parallel-fibered bone dominating throughout the cortex that was preserved.

*Mussaurus* was examined by[S10,S16] and more recently by[S17]. *Mussaurus* contains WPC that falls under the fibrolamellar complex during very early ontogeny. The individuals

examined by Cerda et al.[S10] appear to be late subadults, with MPM-PV 1815 containing more closely spaced growth marks in the outer cortex than specimen MLP 61-III-20-22. However, the more recent study by Pol et al.[S17] shows a transition from the fibrolamellar complex to a woven-parallel complex, with increasing amounts of parallel-fibered bone in the second to largest individual. The presence of large amounts of woven bone in the largest individual studied (MLP 61-111-20-22), however, as well as the variable incidence of growth marks[S10] indicated that more research was required to fully understand the life history of this taxon. Thus, a very recent study by Cerda et al.[S18] examined the humeri, femora and fibulae from 13 *Mussaurus* individuals of different sizes. Growth rates and the incidence of growth marks are variable amongst the specimens such that there is little correlation between ontogeny and body size. Some individuals exhibit WPC through to mid-ontogeny, others exhibit a predominance of parallel-fibered bone. The authors provided several reasons for this variability including sexual dimorphism, developmental plasticity and incorrect taxon identification, with the most likely being developmental plasticity[S18]. *Mussaurus* is slightly more basal than *Aardonyx* and *Sefapanosaurus*. It is possible that *Mussaurus* had begun to develop inconsistent high growth rates, but this rapid growth had yet to become fixed in this taxon's life history.

The Argentinian lessemsaurids *Lessemsaurus sauropoides* (PVL 6580, PVL 4822/64) and *Ingentia prima* (PVSJ 1086) both contain a highly vascularized fibrolamellar complex in the inner most cortices, becoming a WPC in the mid- and outer cortices[S9,S10]. Despite the *Lessemsaurus* specimens containing four to five LAGs and the *Ingentia* individual eight LAGs, none of the individuals were fully grown (i.e. an EFS is absent). The zones between the LAGs are wide and growth marks are present throughout the cortex in both taxa[S9]. The osteohistology from a giant South African lessemsaurid, *Ledumahadi mafube* (BP/1/7120) shows that the mid-cortex comprises WPC and the outer cortex transitions into parallel-

fibered bone with an EFS[S19]. The growth marks are present in at least the outer third of the cortex. However, the individual represents an almost fully grown adult and the inner cortex is completely remodeled[S19]. Thus, we cannot confirm the presence of growth marks throughout the entire cortex as is seen in *Lessemsaurus* and *Ingentia*. Additionally, comparing this individual with the other lessemsaurids is difficult because *Lessemsaurus* and *Ingentia* represent relatively ontogenetically young individuals (with *Lessemsaurus* PVL 6580 possibly representing a juvenile, see[S9]).

Cerda et al.[S10] also examined the basal eusauropods, *Patagosaurus* and *Volkheimeria*. The *Patagosaurus* specimen, PVL 4075, did not contain an EFS and exhibited "regularly spaced annuli" with no clear reduction in growth mark spacing towards the outer cortex, although from the images the annuli are relatively closely spaced towards the outer cortex. This suggests a late subadult stage for this specimen. Growth marks are present only in the outer cortex. Woven bone is more prominent compared to the more basal sauropodomorphs.

The specimen representing *Volkheimeria* is relatively small, growth marks are rare (an exact number is not given, but at least two are shown in the images) and restricted to the outer cortex and the bone lacks an EFS. The specimen used, PVL 4077, may represent a relatively young individual as shown by the presence of highly vascularized woven bone at the subperiosteal surface, showing that the individual was still actively growing at the time of death. Thus, it is possible that growth marks appeared during mid-ontogeny, but this cannot be confirmed until further material is examined.

Sander et al.[S12] described the osteohistology of *Isanosaurus* from Thailand. Originally considered to be the oldest sauropod, its age is now uncertain and may be anything from Late Triassic to Late Jurassic in age[S6]. The bone tissues of the specimen studied consist of the highly vascularized woven-parallel complex, which Sander et al.[S12] described as laminar fibrolamellar bone tissue. Growth marks and polish lines are absent suggesting uninterrupted

growth until late ontogeny similar to Neosauropoda. However, this characteristic coupled with the lack of Haversian remodeling in the cortex indicates that a relatively young status for this specimen cannot be ruled out[S12] and thus, its life history remains uncertain.

**Supplemental References**

S1. Buffrénil, V. de, Ricqlès, A.J. de, Zylberberg, L., Padian, K. (Eds). 2021. Skeletal histology and paleohistology, CRC Press, New York.

S2. Prondvai, E., Stein, K.H., Ricqlès, A. de., Cubo, J. 2014. Development-based revision of bone tissue classification: the importance of semantics for science. Biological Journal of the Linnean Society, 112, 799–816.

S3. Hutton, J.M. 1986. Age determination of living Nile crocodiles from the cortical stratification of bone. Copeia 332–341.

S4. Stein, K. and Prondvai, E. 2014. Rethinking the nature of fibrolamellar bone: an integrative biological revision of sauropod plexiform bone formation. Biological Reviews of the Cambridge Philosophical Society 89, 24–47. https://doi.org/10.1111/brv/12041

S5. Yates, A.M., Bonnan, M.F., Neveling, J., Chinsamy, A., Blackbeard, M.G. 2010. A new transitional sauropodomorph dinosaur from the Early Jurassic of South Africa and the evolution of sauropod feeding and quadrupedalism. Proceedings of the Royal Society B 277, 787–794. https://doi.org/10.1098/rspb.2009.1440

S6. Stein, K.H.W. 2010. Long bone histology of basalmost and derived Sauropodomorpha: the convergence of fibrolamellar bone and the evolution of gigantism and nanism. PhD dissertation, University of Bonn, Germany, 213pp.

S7. Sander, P.M. and Klein, N. 2005. Developmental plasticity in the life history of a prosauropod dinosaur. Science 310, 1800–1802.

S8. Klein, N. and Sander, P.M. 2007. Bone histology and growth of the prosauropod dinosaur *Plateosaurus engelhardti* von Meyer, 1837 from the Norian bonebeds of Trossingen (Germany) and Frick (Switzerland). Special Papers in Palaeontology 77, 169–206.

S9. Apaldetii, C., Martínez, R.N., Cerda, I.A., Pol, D., Alcober, O. 2018. An early trend towards gigantism in Triassic sauropodomorph dinosaurs. Nature Ecology and Evolution 2(8), 1227–1232. https://doi.org/10.1038/s41559-018-0599-y

S10. Cerda, I.A., Chinsamy, A., Pol, D., Apaldetti, C., Otero, A., Powell, J.E., Martínez, R.N. 2017. Novel insight into the origin of the growth dynamics of sauropod dinosaurs. PLoS ONE 12(6), e0179707. https://doi.org/10.1371/journal.pone.017907

S11. Chapelle, K.E.J., Barrett, P.M., Botha, J., Choiniere J.N. 2019. *Ngwevu intloko*: a new early sauropodomorph dinosaur from the Lower Jurassic Elliot Formation of South Africa and comments on cranial ontogeny in *Massospondylus carinatus*. PeerJ. https://doi.org/10.7717/peerj.7240

S12. Sander, P.M., Klein, N., Buffetaut, E., Cuny, G., Suteethorn, V., Le Loeuff, J. 2004. Adaptive radiation in sauropod dinosaurs: Bone histology indicates rapid evolution of giant body size through acceleration. Organisms Diversity and Evolution 4, 165–173.

S13. Krupandan, E., Chinsamy-Turan, A., Pol, D. 2018. The long bone histology of the sauropodomorph, *Antetonitrus ingenipes*. The Anatomical Record 301, 1506–1518.

S14. Fabrègues de, C.P., Allain, R. 2020. *Kholumolumo ellenbergerorum*, gen. et sp. nov., a new early sauropodomorph from the lower Elliot Formation (Upper Triassic) of Maphutseng, Lesotho. Journal of Vertebrate Paleontology 39(6), e1732996. https://doi.org/10.1080/02724634.2019.1732996

S15. Chapelle, K.E.J., Botha, J., Choiniere, J.N. 2021. Extreme growth plasticity in the early branching sauropodomorph *Massospondylus carinatus*. Biology Letters 17, 20200843. https://doi.org/10.1098/rsbl.2020.0843.

S16. Cerda, I.A., Pol, D., Chinsamy, A. 2014. Osteohistological insight into the early stages of growth in *Mussaurus patagonicus* (Dinosauria, Sauropodomorpha). Historical Biology 26(1), 110–121. http://dx.doi.org/10.1080/08912963.2012.763119

S17. Pol, D., Mancuso, A.C., Smith, R.M.H., Marsicano, C.A., Ramezani, J., Cerda, I.A., Otero, A., Fernandez, V. 2021. Earliest evidence of herd-living and age segregation amongst dinosaurs. Scientific Reports 11, 20023. https://doi.org/10.1038/s41598-021-99176-1

S18. Cerda, I. A., Pol, D., Otero, A., Chinsamy, A. 2022. Palaeobiology of the early sauropodomorph *Mussaurus patagonicus* inferred from its long bone histology. Palaeontology e12614.

S19. McPhee, B., Benson, R, Botha-Brink, J., Bordy, E., Choiniere, J. 2018. A giant dinosaur from the earliest Jurassic of South Africa and the transition to quadrupedality in early sauropodomorphs. Current Biology 28, 3143–3153. https://doi.org/10.1016/j.cub.2018.07.063

S20. Langer, M. C., Ramezani, J., Da Rosa, A. A. S. 2018. U-Pb age constraints on dinosaur rise from south Brazil. Gondwana Research 57, 133–140.

S21. Lallensack, J. N., Teschner, E. M., Pabst, B., Sander, P. M. 2021. New skulls of the basal sauropodomorph *Plateosaurus trossingensis* from Frick, Switzerland: Is there more than one species? Acta Palaeontologica Polonica 66(1), 1–28.

S22. Martínez, R. N., Apaldetti, C., Correa, G., Colombi, C. E., Fernández, E., Santi Malnis, P., Praderio, A., Abelín, D., Benegas, L. G., Aguilar-Cameo, A., Alcober, O. A. 2015. A New Late Triassic Vertebrate Assemblage from Northwestern Argentina. Ameghiniana 52(4), 379–390.

S23. Apaldetti, C., Martinez, R. N., Alcober, O. A., Pol, D. 2011. A New Basal Sauropodomorph (Dinosauria: Saurischia) from Quebrada del Barro Formation (Marayes-El Carrizal Basin), Northwestern Argentina. PLoS ONE 6(11), e26964.

S24. Martínez, R. N. 2009. *Adeopapposaurus mognai*, gen. et sp. nov. (Dinosauria: Sauropodomorpha), with comments on adaptations of basal Sauropodomorpha. Journal of Vertebrate Paleontology 29(1), 142–164.

S25. Bordy, E. M., Abrahams, M., Sharman, G. R., Viglietti, P. A., Benson, R. B. J., McPhee, B. W., Barrett, P. M., Sciscio, L., Condon, D., Mundil, R., Rademan, Z., Jinnah, Z., Clark, J. M., Suarez, C. A., Chapelle, K. E. J., Choiniere, J. N. 2020. A chronostratigraphic framework for the upper Stormberg Group: Implications for the Triassic-Jurassic boundary in southern Africa. Earth-Science Reviews 103120.

S26. Apaldetti, C., Martinez, R. N., Pol, D., Souter, T. 2014. Redescription of the skull of *Coloradisaurus brevis* (Dinosauria, Sauropodomorpha) from the Late Triassic Los Colorados Formation of the Ischigualasto-Villa Union Basin, northwestern Argentina. Journal of Vertebrate Paleontology 34(5), 1113–1132.

S27. Kent, D. V., Santi Malnis, P., Colombi, C. E., Martínez, R. N. 2014. Age constraints on the dispersal of dinosaurs in the Late Triassic from magnetochronology of the Los Colorados Formation (Argentina). Proceedings of the National Academy of Sciences 111(22), 7958–7963.

S28. Pol, D., Garrido, A., Cerda, I. A. 2011. A new sauropodomorph dinosaur from the Early Jurassic of Patagonia and the origin and evolution of the sauropod-type sacrum. PLoS ONE 6(1), e14572.

S29. Cúneo R., Ramezani, J., Scasso, R., Pol, D., Escapa, I., Zavattieri, A. M., Bowring, S. A. 2013. High-precision U–Pb geochronology and a new chronostratigraphy for the Cañadón Asfalto Basin, Chubut, central Patagonia: Implications for terrestrial faunal and floral evolution in Jurassic. Gondwana Research 24, 1267–1275.

S30. Racey, A., Goodall, J. G. S. 2009. Palynology and stratigraphy of the Mesozoic Khorat Group red bed sequences from Thailand. In: Buffetaut, E. Curry, G. le Loeuff, J., Suteethorn, V. (Eds.), Late Palaeozoic and Mesozoic ecosystems in SE Asia. Geological Society, London, Special Publications, 69–83.

S31. Benson, B.J., Hunt, G., Carrano, M.T., Campione, N. 2018. Cope's Rule and the adaptive landscape of dinosaur body size evolution. Palaeontology 61(1), 13–48.

S32. Apaldetti, C., Pol, D., Ezcurra, M.D., Martínez, R.N. 2021. Sauropodomorph evolution across the Triassic-Jurassic boundary: body size, locomotion, and their influence on morphological disparity. Scientific Reports 11, 22534.

S33. Campione, N.E., Evans, D.C., Brown, C.M., Carrano, M.T. 2014. Body mass estimation in non-avian bipeds using a theoretical conversion to quadruped stylopodial proportions. Methods in Ecology and Evolution, 5(9), 913–923.

## Supplemental Figures

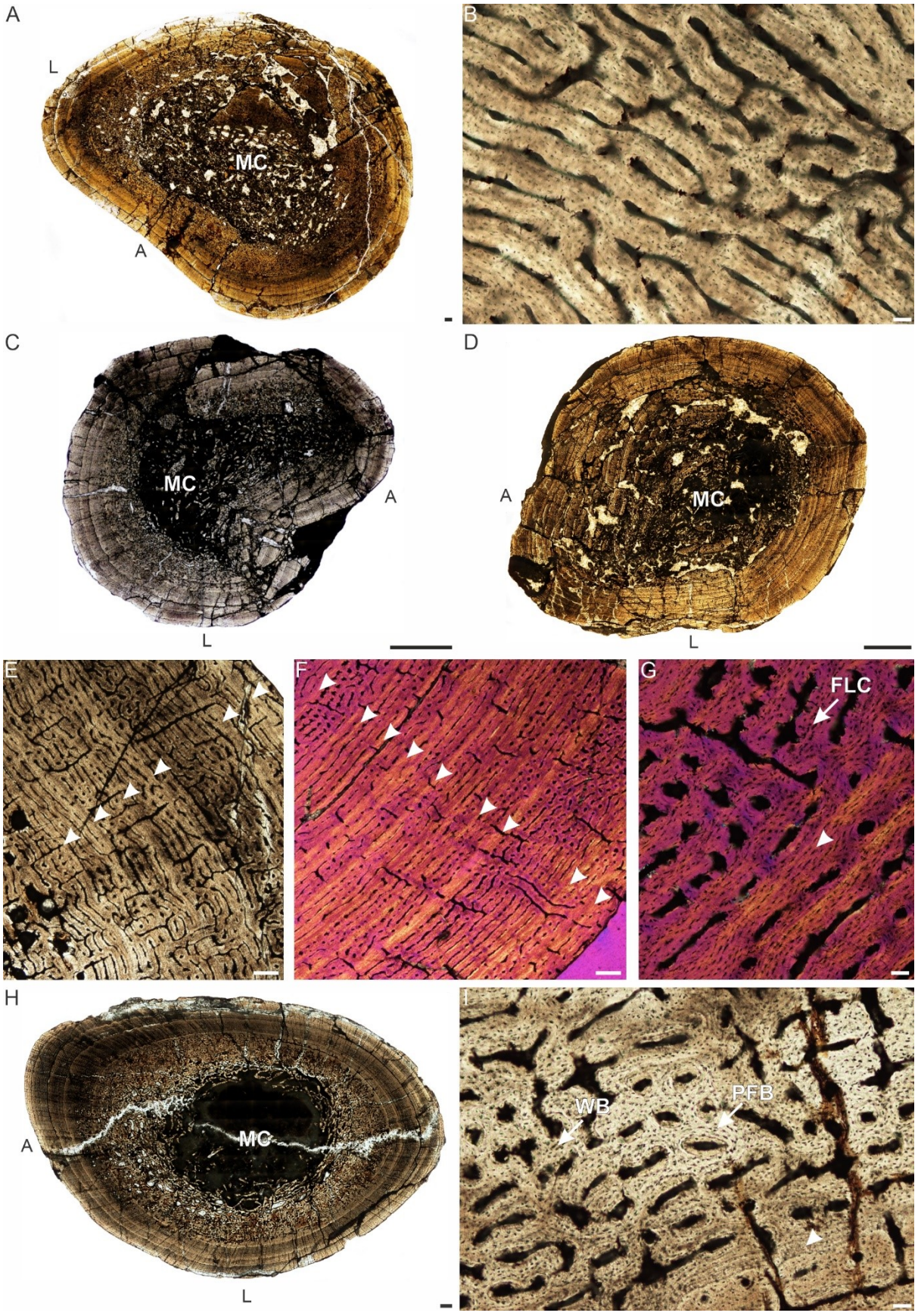

Supplementary Figure 1. Osteohistology of *Sefapanosaurus* elements. A, overall transverse section of humerus BP/1/7434. B, high magnification of the fibrolamellar complex in the humerus. C, overall transverse section of radius BP/1/7436. D, overall transverse section of radius BP/1/7435. E, BP/1/7435 showing a plexiform vascular arrangement. F, BP/1/7435 showing numerous growth marks in the woven-parallel complex. G, BP/1/7435 showing a high magnification of a fibrolamellar complex. H, ulna BP/1/7437 showing the overall transverse section. I, high magnification of BP/1/7437 showing a rapidly forming woven-parallel complex interrupted by growth marks. Arrowheads indicate growth marks. Scale bars A 1000 µm, C, D 5000 µm, B, G 100 µm, E, F, I 500 µm, H 1000 µm. Abbreviations: A, anterior; L, lateral; MC, medullary cavity; FLC fibrolamellar complex; PFB, parallel-fibered bone; WB, woven bone. Related to STAR Methods.

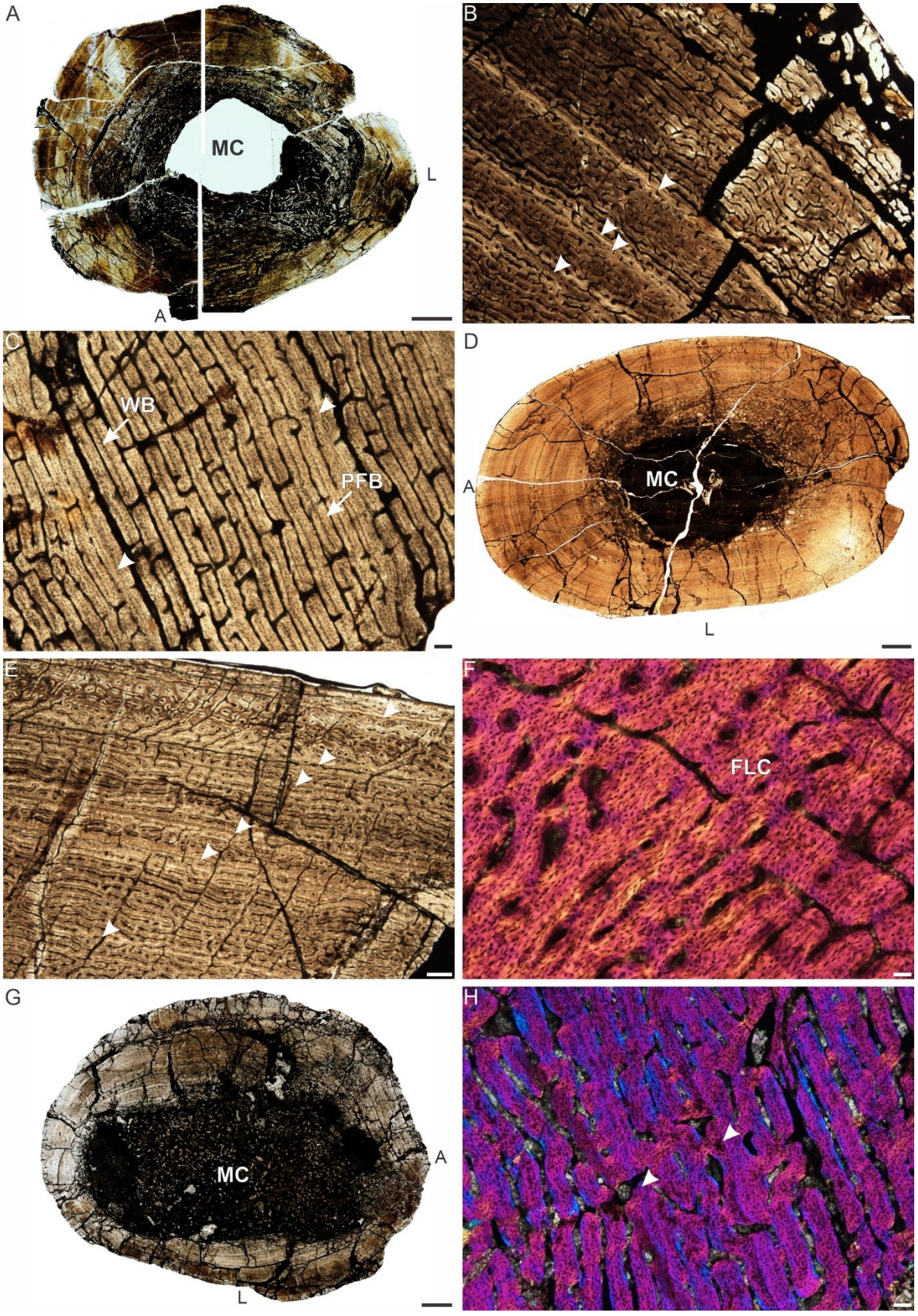
A
MC
L
A
B
C
WB
PFB
D
A
MC
L
E
F
FLC
G
MC
A
L
H

Supplementary Figure 2. Osteohistology of *Sefapanosaurus* elements. A, femur BP/1/7444 showing the overall transverse section. B, BP/1/7444 showing a highly vascularized woven-parallel complex interrupted by growth marks. C, high magnification of BP/1/7444 showing a mixture of woven and parallel-fibered bone to form the woven-parallel complex and a laminar vascular network. D, tibia BP/1/7445 showing the overall transverse section. E, BP/1/7445 high magnification showing a woven parallel complex interrupted by growth marks. F, high magnification of BP/1/7445 showing a highly vascularized fibrolamellar complex. G, fibula BP/1/7446 showing the overall transverse section. H, high magnification of BP/1/7446 showing highly vascularized primary tissues dominated by woven bone. Arrowheads indicate growth marks. Scale bars A, G 1000 µm, D 5000 µm, B, E 500 µm, C, F, H 100 µm. Abbreviations: A, anterior; L, lateral; MC, medullary cavity; PFB, parallel-fibered bone; WB, woven bone. Related to STAR Methods.

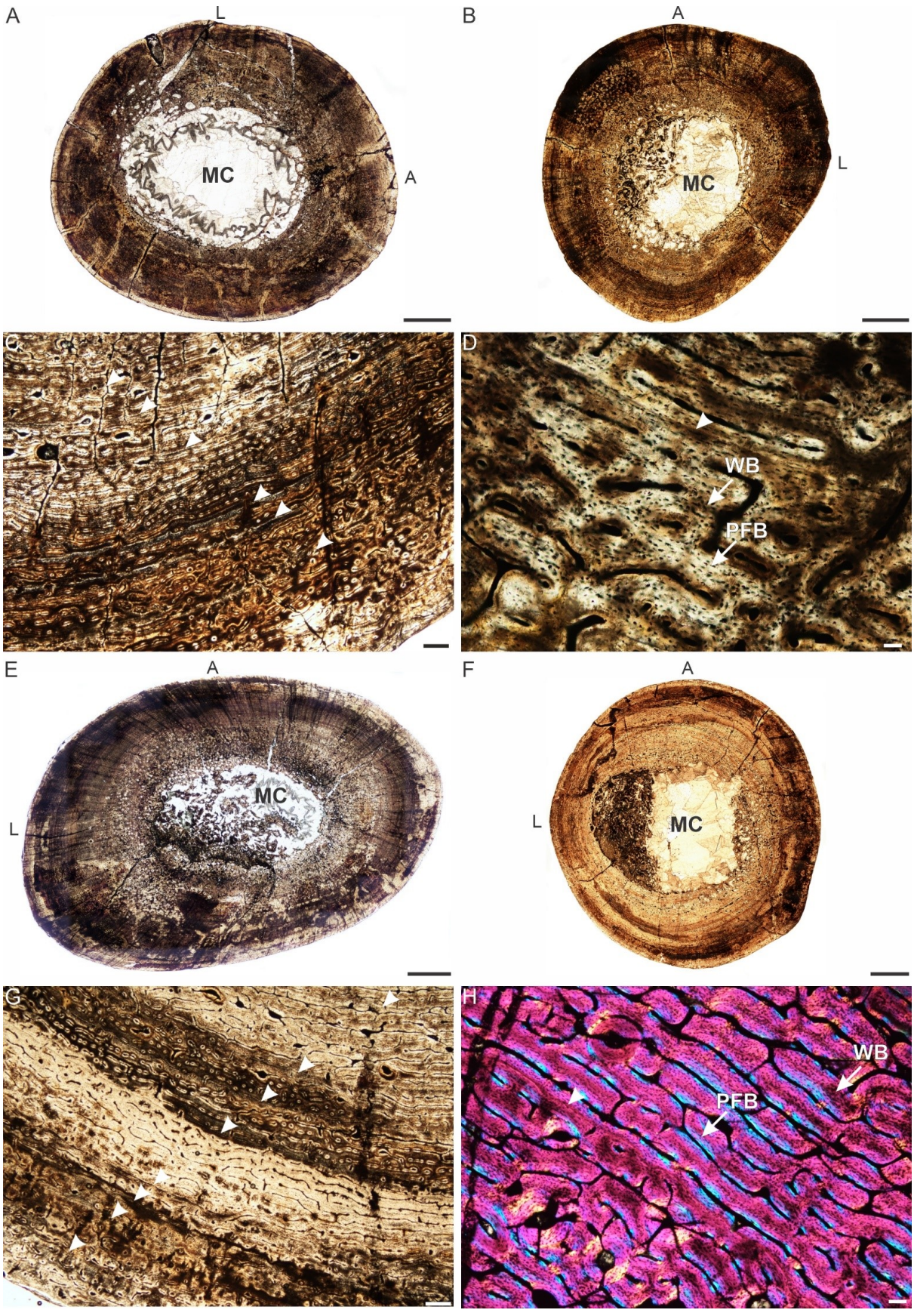
A
L
MC
A
B
A
MC
L
C
D
WB
PFB
E
A
L
MC
F
A
L
MC
G
H
WB
PFB

Supplementary Figure 3. Osteohistology of the *Aardonyx* elements. A, Radius BP/1/5379a showing the overall transverse section. B, radius BP/1/6321 showing the overall transverse section. C, BP/1/6321 showing a woven-parallel complex interrupted by numerous growth marks. D, BP/1/6321 high magnification showing the proportions of woven and parallel-fibered bone. E, ulna BP/1/5379b showing the overall transverse section. F, fibula BP/1/6316 showing the overall transverse section. G, BP/1/6316 woven-parallel complex showing sub-laminar and longitudinally-oriented primary osteons. The woven-parallel complex is interrupted by growth marks. H, high magnification of BP/1/6316 showing the dominance of woven bone. Arrowheads indicate growth marks. Scale bars A, B, E, F 5000 μm, C, G 500 μm, D, H 100 μm. Abbreviations: A, anterior; L, lateral; MC, medullary cavity; PFB, parallel-fibered bone; WB, woven bone. Related to STAR Methods.

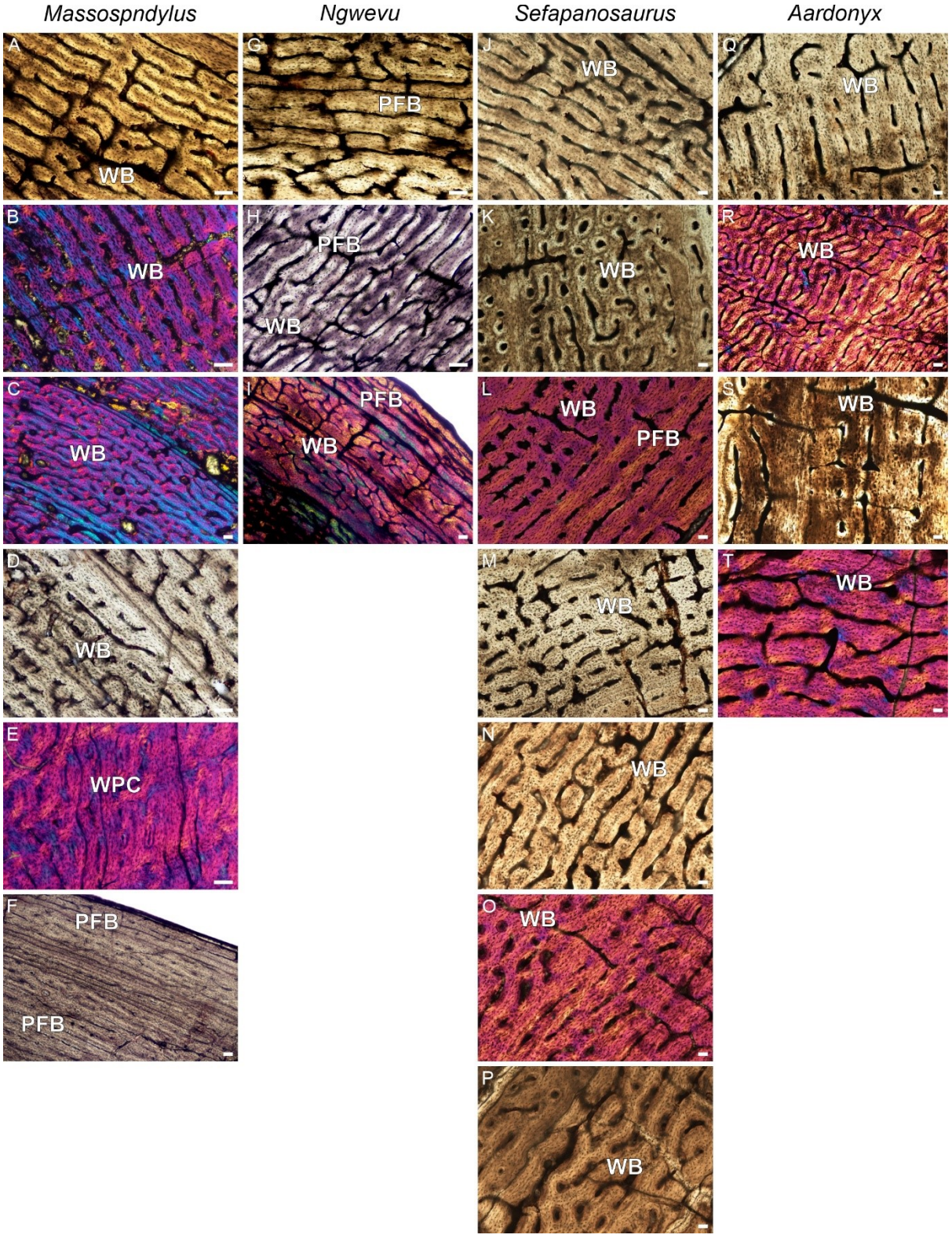
Massospndylus
Ngwevu
Sefapanosaurus
Aardonyx
A
WB
G
PFB
J
WB
Q
WB
B
WB
H
PFB
WB
K
WB
R
WB
C
WB
I
PFB
WB
L
WB
PFB
S
WB
D
WB
M
WB
T
WB
E
WPC
N
WB
F
PFB
PFB
O
WB
P
WB

Supplementary Figure 4. High magnification images of the mid-cortical osteohistology of *Massospondylus* (A–F), *Ngwevu* (G–I), *Sefapanosaurus* (J–P) and *Aardonyx* (Q–T) showing regions of woven-fibered bone. A, tibia BP/1/4376b; B, femur BP/1/5253; C, tibia BP/1/5108b; D, humerus BP/1/4751a; E,F, femur BP/1/4934; G, H, femur BP/1/4779b; I, humerus BP/1/4779a; J, humerus BP/1/7434; K, radius BP/1/7436; L, radius BP/1/7435; M, ulna BP/1/7437; N, femur BP/1/7444; O, tibia BP/1/7445; P, fibula BP/1/7446; Q, radius BP/1/5379; R, ulna BP/1/5379; S, radius BP/1/6321; T, fibula BP/1/6316. A, B, represent juvenile specimens of *Massospondylus*, whereas E, F (outer cortex), represent the adult *Massospondylus* BP/1/4934 shown in[1]. Large portions of woven bone are present during the early ontogenetic stages, which are replaced by parallel-fibered bone in the ontogenetically older individuals. G–I, *Ngwevu* contains a mixture of woven and parallel-fibered bone. J–T show examples of woven bone in *Sefapanosaurus* and *Aardonyx*. Scale bars A–I, R 100 µm, J–T 50 µm. Abbreviations: PFB, parallel-fibered bone; WB, woven bone; WPC, woven-parallel complex. Related to STAR Methods.

**Supplemental Reference**

S1. Cerda, I.A., Chinsamy, A., Pol, D., Apaldetti, C., Otero, A., Powell, J.E., Martínez, R.N. 2017. Novel insight into the origin of the growth dynamics of sauropod dinosaurs. PLoS ONE 12(6), e0179707. https://doi.org/10.1371/journal.pone.017907

Click here to access/download

**Supplemental Videos and Spreadsheets**

Supplementary Table.xlsx